frontiers | Frontiers in Marine Science

TYPE Original Research
PUBLISHED 12 September 2025
DOI 10.3389/fmars.2025.1589660

Check for updates

OPEN ACCESS

EDITED BY
Hans Uwe Dahms,
Kaohsiung Medical University, Taiwan

REVIEWED BY
Joachim Reitner,
University of Göttingen, Germany
Stacy Kim,
Moss Landing Marine Laboratories,
United States

*CORRESPONDENCE
Madeline P. B. C. Anderson
mason@bas.ac.uk

RECEIVED 07 March 2025
ACCEPTED 25 August 2025
PUBLISHED 12 September 2025

CITATION
Anderson MPBC, Reid WDK, Bohrmann G, Dohrmann I, Hollyman PR, Kasten S, Pape T, Römer M, Newton J, Wigham BD and Linse K (2025) The abundance, diversity, and assemblage structure of the macrobenthos at the South Georgia shelf methane seeps. *Front. Mar. Sci.* 12:1589660. doi: 10.3389/fmars.2025.1589660

COPYRIGHT
© 2025 Anderson, Reid, Bohrmann, Dohrmann, Hollyman, Kasten, Pape, Römer, Newton, Wigham and Linse. This is an open-access article distributed under the terms of the Creative Commons Attribution License (CC BY). The use, distribution or reproduction in other forums is permitted, provided the original author(s) and the copyright owner(s) are credited and that the original publication in this journal is cited, in accordance with accepted academic practice. No use, distribution or reproduction is permitted which does not comply with these terms.

The abundance, diversity, and assemblage structure of the macrobenthos at the South Georgia shelf methane seeps

Madeline P. B. C. Anderson[1,2,3]*, William D. K. Reid[2], Gerhard Bohrmann[4,5], Ingrid Dohrmann[6], Philip R. Hollyman[1,7], Sabine Kasten[4,5,6], Thomas Pape[4,5], Miriam Römer[4,5], Jason Newton[3], Ben D. Wigham[2] and Katrin Linse[1]

[1]British Antarctic Survey, Cambridge, United Kingdom, [2]School of Natural and Environmental Sciences, Newcastle University, Newcastle upon Tyne, United Kingdom, [3]National Environmental Isotope Facility, SUERC, East Kilbride, United Kingdom, [4]MARUM – Center for Marine Environmental Sciences, University of Bremen, Bremen, Germany, [5]Faculty of Geosciences, University of Bremen, Bremen, Germany, [6]Alfred Wegener Institute Helmholtz Centre for Polar and Marine Research, Bremerhaven, Germany, [7]School of Ocean Sciences, Bangor University, Menai Bridge, United Kingdom

A quarter of all marine methane, a potent greenhouse gas, is estimated to be hosted in Southern Ocean sediments. Climate change-induced ocean warming and ice shelf melting risk the stability of sedimentary gas hydrates, resulting in potential degassing and establishment of marine methane seeps. While methane seeps can originate from various sources, the destabilisation of gas hydrates may contribute to the formation and persistence of some active seeps. The impact of these seeps and their risks to the diverse sub-Antarctic and Antarctic benthic shelf fauna is uncertain. As a sentinel for change in the sub-Antarctic and wider Antarctic region, this study explores South Georgia's continental shelf macrobenthic methane seep assemblages, for their diversity, richness, and abundance, and their environmental drivers influencing macrofaunal community composition. Seven of South Georgia's shelf troughs hosting active methane seeps were investigated during RV METEOR's M134 expedition in 2017. Species richness at 11 stations ranged from 19–51 species from a total of 103 species discovered across all sites. Station abundance ranged from 3,303–30,326 m^2. Diversity was higher at stations with greater methane- and sulfate-flux, and hydrogen sulfide at 25 cm depth. Abundance and richness were lower where surface sediment had high hydrogen sulfide concentrations. Abundance and species richness were lower at stations dominated by iron-reduction in the sediment. Assemblages were characterized by the presence of Southern Ocean species and by the absence of megafaunal chemosynthetic taxa. Arthropods, mostly crustacean, and annelid species made up three quarters of overall species richness, while molluscan and echinoderm species were depauperate with only 15 species. Compared with Southern Ocean macrobenthic assemblages, the South Georgia seep assemblages from sediments with gas hydrates present in the near-surface showed a lower species richness and change in taxon

composition, also accompanied by lower numbers of calcium-carbonate shell bearing taxa. The current diverse benthic Antarctic biodiversity, especially the diversity of calcifiers, is likely at risk when methane seeps become established on Southern Ocean continental shelves as the reduction in habitat diversity leads to the decline in taxonomic diversity and species richness.

KEYWORDS

hydrocarbon seafloor emission, sub-Antarctic, microbial mats, Polychaeta, remotely operated vehicle (ROV), multicorer samples

Highlights

- Shallow sediment hosted macrofaunal samples collected from active methane seep stations in South Georgia via multicorer for abundance and diversity analysis.
- All taxa detected resemble representatives of the known Southern Ocean macrofauna in soft sediment habitats. No distinct chemosynthetic megafaunal taxa are present.
- Abundances and species richness of the macrofauna are higher at stations with greater methane and sulfate flux, as well as in the presence of in-sediment hydrogen sulfide, however they are lower in the presence of surface sediment hydrogen sulfide.

1 Introduction

Hydrocarbon seeps are areas of the seafloor where reduced chemicals, including methane and hydrogen sulfide, leave marine sediments (e.g., Joye, 2020). Methane is a potent greenhouse gas (Stocker et al., 2014) and can be identified leaving the seafloor in areas where there are high dissolved concentrations in the water column, evidence of gas flares or bubble plumes, or the presence of subsurface bottom simulating reflectors (e.g., Åström et al., 2019; Fischer et al., 2012; Joye, 2020). Methane emitted from the seafloor can be the result of thermogenic breakdown of organic matter (e.g., Stolper et al., 2014), or the biological production of methane in anoxic marine sediment by methanogens (e.g., Stolper et al., 2014; Whiticar, 1999). The presence of methane in sediment can drive microbial/biogeochemical processes by serving as a substrate for chemosynthetic primary production, thereby supporting the benthic food web (e.g., Åström et al., 2019). Methane flux within the sediment can have significant implications on microbial and metazoan assemblage composition, impacting both the biogeochemical cycling in the sediment and regional biodiversity on a series of different scales (Ashford et al., 2021a; Levin, 1992). An estimated 25% of all marine methane is in Southern Ocean sediments (Thurber et al., 2020). Understanding the presence, stability, and fate of methane in marine sediments is crucial for elucidating its role in shaping Southern Ocean biodiversity, particularly in the context of a warming climate.

Methane seeps occur on active and passive continental margins and are found from shallow waters to the deep sea (e.g., Åström et al., 2018; Fischer et al., 2012, 2013; Judd, 2003; Nöthen and Kasten, 2011; Thurber et al., 2020) and have been discovered in all major oceans including along the Northeastern Pacific margin (e.g., Bohrmann et al., 2002b; Levin et al., 2010), the New Zealand margin (e.g., Thurber et al., 2013), off Costa Rica (e.g., Bohrmann et al., 2002a; Levin et al., 2015), the Black Sea (e.g., Römer et al., 2012; Mazzini et al., 2008), Mediterranean Sea (Römer et al., 2014a), the Arabian sea (e.g., Fischer et al., 2012) and the Arctic (e.g., Åström et al., 2020). In the western Svalbard Arctic margin, methane seeps have been the focus of studies on seasonal seep activity, influenced by inflows of seasonal bottom waters (Åström et al., 2016; Ferré et al., 2012; Myhre et al., 2016; Portnov et al., 2016).

Methane seeps typically form a mosaic of distinct habitats on the seafloor (Fischer et al., 2012; Levin, 1992), characterized by localized increases in biomass and the abundance of specific microbial and metazoan taxonomic groups compared to the surrounding sediment (Ashford et al., 2021b; Levin, 1992). Microbial and geochemical processes, such as anaerobic methane oxidation and sulfate reduction, drive geochemical gradients and fluxes that influence habitat formation, ultimately shaping the composition of meio-, macro-, and megafaunal assemblages at these sites. Methane seeps are characterised by the anaerobic oxidation of methane (AOM), carried out by a consortium of Archaea and sulfate-reducing bacteria, which produce hydrogen sulfide and bicarbonate (e.g., Boetius et al., 2000; Hinrichs et al., 1999; Hoehler et al., 1994). While methane is a key driver, it is the resulting geochemical processes, specifically the downward diffusion of seawater sulfate and the upward diffusion of methane, that govern AOM. This interplay leads to the formation of a typical sulfate/methane transition (SMT), where both sulfate and methane become depleted (e.g., Iversen and Jorgensen, 1985; Niewöhner et al., 1998; Treude et al., 2005). The process of AOM produces hydrogen sulfide at the SMT from where sulfide diffuses both downward and upward. It can reach the shallow sediments close to the sediment surface where metazoans would typically occur. Other compounds found at methane seeps, such as ammonium,

further contribute to the toxicity and physiological challenges faced by many species. As a result, methane seep habitats are defined by steep geochemical gradients, shaping metazoan assemblages that are either tolerant of high sulfide levels or capable of exploiting free methane. Seep megafauna, including tubeworms and vesicomyid clams, have adapted to these conditions as a result of symbiotic relationships with sulfide- or methane-oxidizing bacteria, to generate energy for growth and reproduction. Metazoans including macrofaunal bivalves such as thyasirids, and polychaetes such as Cirratulidae, Hesionidae, Orbiniidae and Ampharetidae have the physiological adaptations to live in these habitats and feed on the sulfide oxidising bacterial mats (e.g., Levin et al., 2000; Vetter and Dayton, 1998; Washburn et al., 2018). Specialised fauna such as tube worms and vesicomyid clams are typically associated with high concentrations of methane and hydrogen sulfide at deep sea methane seep sites (Arrázola and Acosta, 2024; Sahling et al., 2003). More generalist or opportunistic polychaete and bivalve taxa, also found at seeps, may be more tolerant to more moderately reducing conditions in comparison with the specialised fauna (Ashford et al., 2021b). This can create heterogenous patches of metazoan assemblages along methane and hydrogen sulfide gradients in the sediment (Arrázola and Acosta, 2024).

Methane seep habitats are not uniform across spatial and temporal scales, and metazoan assemblage composition varies across locations, influenced by differences in substrate type and sediment geochemistry. For example, in the Gulf of Mexico, metazoan assemblages are dominated by vestimentiferan tubeworms and bathymodiolin mussels (Cordes et al., 2007). In Monterey Bay, California, vesicomyid clams dominate, alongside other seep fauna such as galatheid crabs, solemyid crabs, vestimentiferan worms, columbellid snails, and pyropeltid limpets (Barry et al., 1996). In New Zealand, methane seep habitats are dominated by vestimentiferan tubeworms, vesicomyid clams, and bathymodiolin mussels but also contain unique soft sediment areas dominated by ampharetid polychaetes (Bowden et al., 2013; Sommer et al., 2010). Soft sediment areas dominated by ampharetids and other reducing sediment associated macrofauna are often seen as transitional areas between high methane seeps stations or early successional stages as seep ecosystems develop (Arrázola and Acosta, 2024; Bowden et al., 2013). Alternatively, these taxa have been hypothesised to be more prevalent at shallow methane seeps as a result of the interplay between the availability of chemosynthetic and photosynthetic primary production (Levin, 2005; Sahling et al., 2003). Unlike deep-sea methane seeps, the succession of assemblages in these shallow-water seeps as the methane seep becomes more established is not clearly understood. Shallow water soft sediment methane seep-associated macrofaunal taxa (which may include taxa such as Maldanidae, Ampharetidae and Lumbrineridae) may resemble key taxa found in oxygen minimum zones, whale falls, sewage outflows, and high organic carbon sediments near fish farms. These shallow water methane seep faunal assemblages remain poorly understood yet may be more widespread than currently realised.

The Southern Ocean encompasses regions south of the Polar Front, and far less is known about its methane seeps compared to those in other major oceans. Initial investigations in the Southern Ocean identified potential areas of active methane seeps based on bottom-simulating reflectors north of King George Island (Nakayama et al., 2011; Whiticar and Suess, 1990), South Shetland Islands (Workman et al., 2024), and beneath the Larsen B ice shelf on the Eastern Antarctic Peninsula based on video evidence of dead vesicomyid clam shells (Niemann et al., 2009; Linse et al., 2020). The first clear evidence of active methane seeping came with identification of methane flares, bacterial mats and methane rich sediments at South Georgia (Geprägs et al., 2016; Römer et al., 2014b), Scotia Sea, and quantifying methane in the sediments within the north western Weddell Sea (del Valle et al., 2017). In the shallow waters of the Ross Sea, Thurber et al. (2020) not only reported the discovery of the first shallow water methane seep on the Antarctic continental shelf but also documented the transition from a non-seep to a methane seep environment, including the associated changes in the microbial assemblage. Even though methane seep locations have been identified in the Antarctic and sub-Antarctic, we still know very little regarding the metazoan assemblages associated with them and what is driving assemblage composition.

South Georgia is a Southern Ocean biodiversity hotspot; the South Georgia continental shelf is one of the most speciose regions of the Southern Ocean and is vulnerable to climate change due to geographic location with any regional warming having potentially severe implications on the benthos (Hogg et al., 2011). Active methane seeps have been established on the continental shelf with ikaites (a mineral form of calcium carbonate, sometimes associated with methane presence) discovered on the southern South Georgia shelf (Belchier, 2004). Subsequent studies have detected methane flares at numerous locations on both the northern and southern continental shelf, especially in the shelf troughs (Bohrmann, 2013; Bohrmann et al., 2017; Römer et al., 2014b) and gas hydrates have been recovered from Church Trough on the northern shelf and from Annenkov Trough - West on the southern shelf (Figure 1) (Bohrmann et al., 2017). The predominant source of methane at sites in the Cumberland Bay and in the so-called cross-shelf Trough 6, both situated on the South Georgia shelf, is biogenic in origin (Geprägs et al., 2016; Römer et al., 2014b). Microbial studies have shown electron availability (namely Royal and Church Troughs having sulfide-rich sediments and Cumberland Bay fjord with iron-rich sediments) shapes the ANME assemblage composition (Schnakenberg et al., 2021). Sulfate reduction dominates in Church Trough, while iron reduction was prevalent at Annenkov Trough, Cumberland Bay, and Drygalski Fjord, however concurrent sulfate reduction may be occurring (Wunder et al., 2021). Unlike sulfate, which may be microbially transformed into hydrogen sulfide (toxic to some benthic microbes and metazoa), iron reduction does not produce a toxic compound, and its presence can mitigate sulfide toxicity. This interplay between iron and sulfate availability underpins the microbial assemblage structures across the South Georgia shelf, but the effect on metazoan assemblages is unknown.

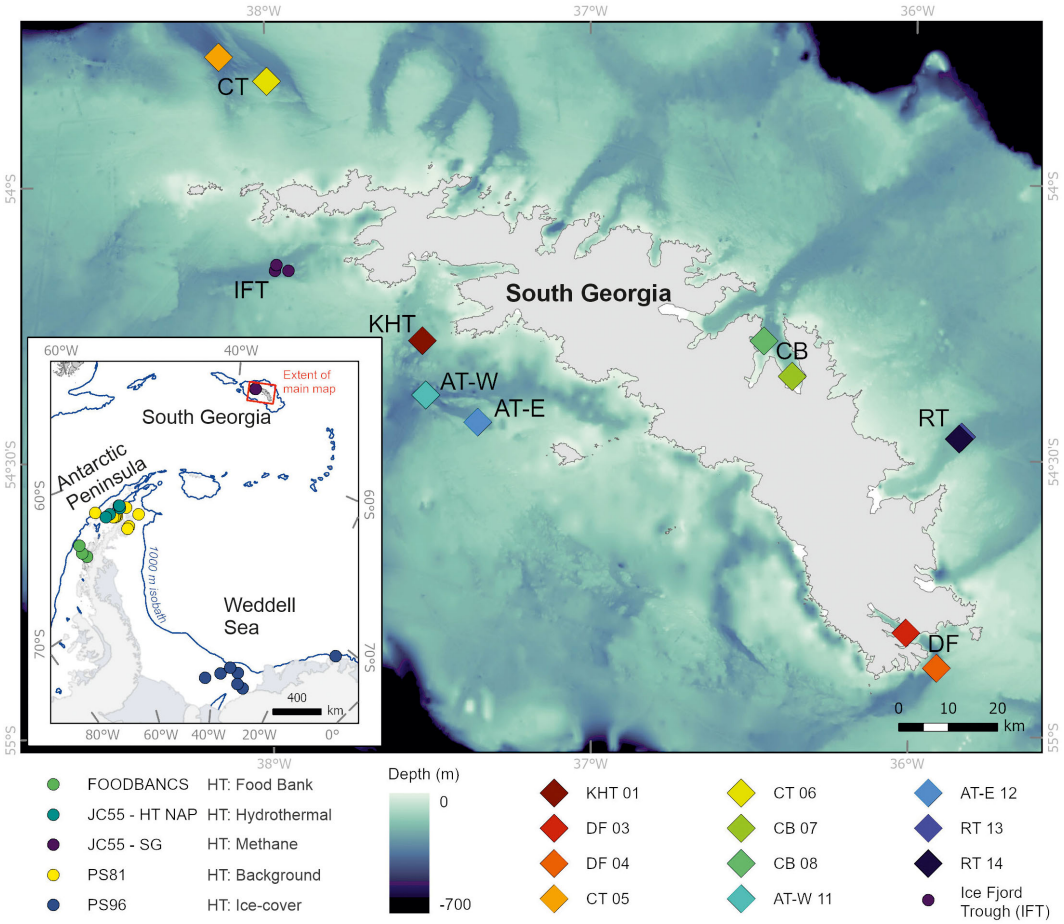

FIGURE 1
Map of South Georgia (SG) with the M134 multicore (MUC) stations plotted and labelled as bio-numbers. In order of GeoB station number; KHT, King Haakon Trough (GeoB22002-2); DF, Drygalski Fjord (GeoB22012–3 and GeoB22015-1); CT, Church Trough (GeoB22031–1 and GeoB22034-3); CB, Cumberland Bay (GeoB22041–2 and GeoB22046-1); AT-W, Annenkov Trough West (GeoB22051-1); AT-E, Annenkov Trough East (GeoB22054-2); RT, Royal Bay Trough (GeoB22062–1 and GeoB22063-1). Inset is the Antarctic Peninsula; Weddell Sea and Scotia Sea region, and includes South Georgia. Inset stations are from additional soft-sediment Southern Ocean expeditions. HT, Habitat Type. FOODBANCS (habitat type: food bank stations), JC55 - HT NAP = Hydrothermal Northern Antarctic Peninsula (habitat type: hydrothermal influenced stations), JC55 - SG (habitat type: methane influenced stations), PS81 (habitat type: background ice cover stations), PS96 (habitat type: ice covered stations). Bathymetry was from Hogg et al. (2015) and coastline was from the SCAR Antarctic Digital Database, 2024. The 1000 m isobath on the peninsula map is extracted from IBCSO (Dorschel et al., 2022). Map produced by the Mapping and Geographic Information Centre, British Antarctic Survey.

In this study, we explore the macrobenthic assemblages collected by multicorer (MUC) from methane seep sediments at 11 locations around the South Georgia continental shelf. Focused sampling on active seeps was possible with imaging systems searching for active bubbling and bacterial mats. The objectives of this study were to (1) examine the diversity and richness of methane seep assemblages on the South Georgia shelf (2) investigate the assemblage composition of the macrobenthos at the phylum and morphospecies level, and (3) assess how the assemblage composition is driven by environmental variables. Additionally, (4) we place the South Georgia methane seep assemblages into the context of other Southern Ocean infaunal assemblages from soft-sediment habitats across a spectrum of potential environmental conditions.

2 Materials and methods

2.1 Study area and expedition

South Georgia is a sub-Antarctic island located in the Scotia Sea, south of the Polar Front and is in the path of the Antarctic Circumpolar Current (Young et al., 2011). At approximately 3,900 km^2 in area, with a surrounding continental shelf of 50–150 km width, South Georgia is characterised by its complex geology (due to tectonic convergence, diverse rock formations, and intense deformation from folding, faulting, and metamorphism) and extensive glacial coverage (Hodgson et al., 2014). The island's geological and glacial history have significantly influenced the island and shelf, including the formation of prominent shelf troughs (Graham et al., 2017; Hodgson et al., 2014),

which shape the bathymetry and sediment distribution (Figure 1). The influence of past glacial advance and retreat is particularly evident in King Haakon Trough, where sediment deposition has been shaped by meltwater runoff, shifting ocean currents, and climate-driven changes in the Southern Hemisphere Westerlies and the Antarctic Circumpolar Current (Lešić et al., 2024; Streuff et al., 2024) and in the glacimarine sediments of Drygalski Fjord (Lešić et al., 2022). The fjords and channels surrounding the island exhibit distinct oceanographic characteristics, including variations in temperature, salinity, and circulation, which are influenced by fjord bathymetry. These oceanographic conditions likely play a key role in structuring macrobenthic assemblages by influencing species distribution and assemblage composition through variations in sedimentation rates, nutrient availability, and habitat heterogeneity. However, detailed oceanographic studies are largely limited to Cumberland Bay (Zanker et al., 2024).

The RV METEOR expedition M134, conducted in January and February 2017, aimed to take a multidisciplinary approach to studying methane emissions from cross-shelf troughs around South Georgia. Using a range of sampling techniques, the survey investigated seven of the at least 10 identified trough systems (Römer et al., 2014b), from the water column to the sediments, to assess the distribution, quantification, and sources of active methane seepage in sub-Antarctic waters (Figure 1) (Bohrmann et al., 2017).

2.2 Sample locations and remotely operated vehicle observations

Station work at gas emission sites were selected following hydroacoustic flare imaging, which were detected using a KONGSBERG EM710 and a PARASOUND P70 echosounder (Bohrmann et al., 2017). All MUCs were collected at active methane seep stations.

The light work-class Remotely Operated Vehicle (ROV) MARUM-SQUID (SAAB Seaeye, UK) was deployed to image and survey the seafloor of the South Georgia cross-shelf troughs in areas of detected gas emissions (Figure 2, Supplementary Materials 1). MARUM-SQUID was equipped with five cameras, the main working camera is a pan-and-tilt mounted Insite Pacific MiniZEUS MKII full HD camera with 2.38-megapixel resolution. Two Imenco Dusky Shark line lasers project two parallel beams at 30 cm distance for size measurements on the seafloor. Benthic habitats were observed by *in-situ* imagery (Supplementary Materials 1). Representative *in-situ* stills of the sites were collected for the comparison of the habitats. The observation of bacterial mats or gas bubbles released from the surface of the sediment may indicate the presence of seeps.

2.3 Water column measurements, seafloor sampling, and pore-water analyses

Oceanographic data were collected using RV METEOR's 24 times 10 l Niskin bottles rosette with a Seabird CTD equipped with conductivity, temperature, pressure, and an SBE 43 dissolved oxygen sensor. The near seafloor (1.8-13.6 m above seafloor) water data were used to report bottom temperature, salinity, and oxygen.

The locations of the MUC stations were determined using seafloor images, such as those in Figure 2. Cores of seafloor sediments and macrobenthic assemblages were obtained with a multicorer (MUC) (Table 1). A 12-core MUC (OKTOPUS GmbH, Kiel, Germany), with eight plastic coring tubes with 95 mm diameter and four plastic coring tubes with 62 mm diameter (all 60 cm in length), was used to collect samples for assessing macrofaunal assemblage structure and geochemical analysis of the potential active methane seep sites. On arrival on deck all cores were photographed to record sediment height, layering and colour, and distributed for later geochemical, sediment and biological analyses (Bohrmann et al., 2017). Water depth of sediment recovery ranged from the shallowest at a Cumberland East Bay station at 136 m (CB 07) to the deepest station at Church Trough 369 m (CT 05) (Table 1).

Per MUC, one core was used for the analysis of *ex situ* concentrations of dissolved methane and one for pore water geochemistry. For methane analysis sediment was sampled in 1 or 2 cm intervals throughout the core and prepared according to a modified headspace gas technique (Kvenvolden, 1986) as described in Pape et al. (2014). The gas samples were analysed onboard for their methane concentrations with a two-channel 6890N (Agilent Technologies) gas chromatograph. Pore water was retrieved from MUC cores using rhizon samplers according to the procedure described by Seeberg-Elverfeldt et al. (2005). Dissolved inorganic carbon (DIC) was analysed on board as described by Hall and Aller (1992). Shore-based analyses were conducted for the concentrations of ammonium, chloride, iron, phosphate, sulfate, and silicate. Sulfate and chloride were determined by means of ion chromatography using a METROHM 930 Compact IC Flex. Ammonium, phosphate and silicate concentrations were analysed using a QuAAtro Continuous Segmented Flow Analyzer (Seal Analytical). Hydrogen sulfide concentrations were measured spectrophotometrically following the methylene blue method after (Cline, 1969) using a DR2800 spectrophotometer (Hach Lange). Fe2+ pore-water concentrations were analysed by inductively coupled plasma optical emission spectrometry by means of a Thermo Scientific iCAP™ 7400 ICP-OES Analysator.

MUC cores per deployment not required for geochemistry and sedimentology were used for macrobiology, ranging from one to five cores and six or 10 cm diameter per station (Table 1 and Anderson et al., 2025). Mobile macrofauna visible on the top of cores were fixed individually in 96 vol-% ethanol. Macrobiology allocated MUC cores (a total of 38) were sliced at 0–2 cm and 2–5 cm horizons using a core extruder, sieved on deck through a 500 µm sieve in ambient temperature of 2-5°C, and fixed in 96 vol-% ethanol.

2.4 Quantitative analyses of South Georgia megabenthic assemblages

Benthic specimens were initially sorted on board to higher taxon level under a Meiji stereomicroscope, and later sorted to

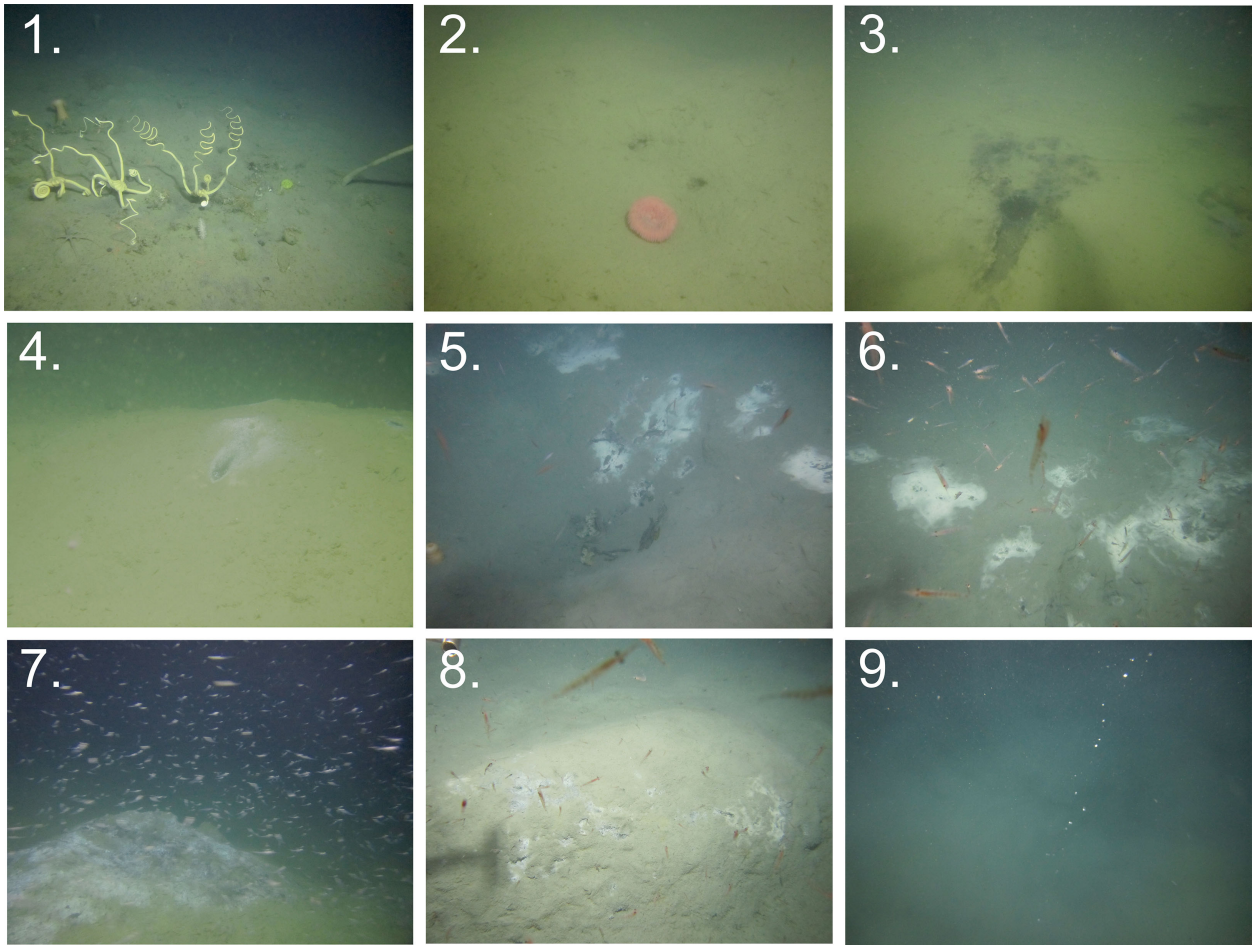

FIGURE 2
ROV images of the seafloor from M134. From left to right, top to bottom, 1. Brittle stars, homogenous looking sediment. Dive22, Ice Fjord Trough (GeoB22010-1). 2. Anemone, with visible orifices. Dive 22, Ice Fjord Trough(GeoB22010-1). 3. Dark sediment dispersed with light coloured sediment. Dive 28, Annenkov Trough- West (GeoB22050-1). 4. Bacterial dusting around an orifice on sediment ridge. Dive 22, Ice Fjord Trough (GeoB22010-1). 5-7. Increasingly large bacterial mats, with increasingly greater number of krill. 5 and 6 Dive 25, Church Trough (GeoB22033-1), 7 Dive 23, Church Trough (GeoB22026-1). 8. Mount with white bacterial mat, bubble in the top left corner. Dive 27, Cumberland Bay (GeoB22047-1). 9. Ebullition in the water column originating from seep. Dive 24, Church Trough (GeoB22029-1). Details about dives are in Supplementary Materials 1.

TABLE 1 Details of the 2017 M134 MUC and CTD locations with GeoB numbers (GeoB No.) and equivalent Station Numbers (Station No.).

Station	GeoB No.	Location	Date (dd.mm)	Instrument	Station No.	Start Latitude (°S)	Start Longitude (°W)	Station Depth (m)
KHT 01	22002-1	King Haakon Trough	21.01	CTD-2	110-1	54°17.238	37°31.302	231
KHT 01	22002-2	King Haakon Trough	21.01	MUC-1	110-2	54°17.245	37°31.328	230
DF 03	22012-1	Drygalski Fjord	24.01	CTD-5	120-1	54°48.871	36°0.598	217
DF 03	22012-3	Drygalski Fjord	24.01	MUC-3	120-3	54°48.873	36°0.604	217
DF 04	22013-1	Drygalski Fjord	24.01	CTD-6	121-1	54°51.270	35°54.659	319
DF 04	22015-1	Drygalski Fjord	25.01	MUC-4	123-1	54°51.269	35°54.667	318
CT 05	22025-1	Church Trough	27.01	CTD-15	133-1	53°46.194	38°8.387	368

(Continued)

10.3389/fmars.2025.1589660

TABLE 1 Continued

Station	GeoB No.	Location	Date (dd.mm)	Instrument	Station No.	Start Latitude (°S)	Start Longitude (°W)	Station Depth (m)
CT 05	22031-1	Church Trough	29.01	MUC-5	139-1	53°46.209	38°8.413	367
CT 06	22034-3	Church Trough	30.01	MUC-6	142-3	53°48.849	37°59.655	211
CB 07	22023-1	Cumberland Bay	26.01	CTD-14	131-1	54°21.110	36°22.424	135
CB 07	22041-2	Cumberland Bay	01.02	MUC-7	149-2	54°21.106	36°22.439	136
CB 08	22021-1	Cumberland Bay	26.01	CTD-12	129-1	54°17.275	36°27.298	144
CB 08	22046-1	Cumberland Bay	03.02	MUC-8	154-1	54°17.270	36°27.710	142
AT-W 11	22049-1	Annenkov Trough - West	05.02	CTD-22	158-1	54°23.152	37°30.764	368
AT-W 11	22051-1	Annenkov Trough - West	05.02	MUC-11	160-1	54°23.152	37°30.765	358
AT-E 12	22054-1	Annenkov Trough - East	07.02	CTD-25	163-1	54°26.156	37°21.083	260
AT-E 12	22054-2	Annenkov Trough - East	07.02	MUC-12	163-2	54°26.169	37°21.094	256
RT 13	22062-1	Royal Trough	09.02	MUC-13	171-1	54°27.454	35°50.668	226
RT 14	22040-1	Royal Trough	31.01	CTD-20	148-1	54°27.685	35°51.138	222
RT 14	22063-1	Royal Trough	23.01	MUC-14	172-1	54°27.695	35°51.142	223

Station depth represents the seafloor depth at the station.

morphospecies level and counted on land under a Zeiss Stemi SV6 stereomicroscope. Individual species were photographed by ScopeTek ScopePhoto 3.1.475. For higher-level taxonomic identifications, we used Arntz and Rauschert's Antarctic Macrobenthos (2015) and taxon specific literature for determination to family, genus and species. Specimens were designated to morphospecies, based on recognisable, unequivocal, morphological features, and their photographs and identifications provided to taxonomic experts for quality control. Morphospecies are addressed as species from here. Due to challenges in identification of Nematoda following fixation, the Nematoda were grouped into a single taxa. The abbreviation 'indet.' was used to denote an indeterminate specimen. Specimens were counted from the 0–2 cm and 2–5 cm horizons of each MUC core. Only partial individuals with heads were counted to avoid duplication. Counts were organized into a quantitative data table, with species as columns and combined identifiers of MUC number, core number, and horizon depth as rows. Core diameter (6 cm or 10 cm) was also recorded for each sample and abundance data were scaled to individuals per m^2 for quantitative analyses between different core sizes. Patterns in species richness, abundance, and diversity were determined by pooling multiple cores from each MUC to obtain an

TABLE 2 Physico-chemical properties (T, S, dissolved O_2) of near-seafloor water recorded during CTD stations.

Station	Station Depth (m)	Altitude (m)	Temperature (°C)	Salinity	Oxygen (mL L^{-1})
KHT 01	231	5.7	1.4267	34.29	4.86
DF 03	217	8.8	1.0282	33.98	6.28
DF 04	319	5.7	1.0408	34.20	5.41
CT 05	308	3.9	1.669	34.40	4.51
CB 07	135	9.6			
CB 08	144	13.6	0.7311	33.94	7.06
AT-W 11	368	1.8	1.87	34.43	4.12
AT-E 12	260	4.2	1.43	34.29	4.61
RT 14	222	9.5	1.18	34.24	5.39

Station depth refers to the depth of the seafloor, while Altitude indicates the height above the seafloor where the CTD was collected. KHT, King Haakon Trough; DF, Drygalski Fjord; CT, Church Trough; CB, Cumberland Bay; AT-W, Annenkov Trough – West; AT-E, Annenkov Trough – East; RB, Royal Bay Trough; NA, Blank cells not available as these samples were not collected.

assemblage per station following the approach of Bell et al. (2016b). Abundances were then summed to phylum level to allow clearer visualisation of broad-scale community patterns. Species richness was checked with a species accumulation curve to test if richness was a result of actual species richness, and not a feature of sampling effort (Supplementary Materials 2).

All analyses were conducted in R.4.3.1 (R Core Team, 2024). All assemblage analyses were conducted using the vegan package (Oksanen et al., 2024). Figures were plotted with ggplot2 and the viridis colour palette, both part of the tidyverse (Wickham et al., 2019). All code used in the analysis of this study is open access at (Anderson, 2025).

Four key diversity indices were calculated for our seep assemblages: species richness, Pielou's Evenness (Pielou, 1966), Shannon-Wiener index (Shannon, 1948; Oksanen et al., 2024) and the Inverse Simpson's index (Simpson, 1949; Oksanen et al., 2024). Species richness provides us with the number of species present at each station and is highly dependent on sampling effort. The Pielou's Evenness was calculated to assess how evenly individuals are distributed among the species at each station and relies on the number of species, and as such can therefore be impacted by sampling effort. The Shannon-Wiener and Inverse Simpson Indices are our measures of alpha diversity. The Shannon-Wiener index (ranging between 0 and 6.69 (the maximum value is loge(number of species))) was selected as it combines the species richness and evenness, thus providing a measure of diversity that incorporates the presence and abundance of rare species. The Inverse Simpson's Index (ranging from 0 to infinity) was used to assess common species within the assemblages, with higher values indicating greater diversity. This provides a different perspective on assemblage structure compared to the Shannon-Wiener index. The effect of sampling effort is less for diversity indices such as the Shannon-Wiener index and inverse Simpson index, as the compound diversity indices have a lower dependence on sampling effort (Magurran, 2003).

Non-metric multidimensional scaling (NMDS) was chosen as the ordination method because it maximises the rank-order correlation between samples in the plot. Each core was kept separate to identify small-scale differences in assemblage structures (Montagna et al., 2017), scaled abundances (m^{-2}) were used. To determine the most suitable dataset for the ordination we ran a procrustes analysis followed by a species cluster stability assessment. The procrustes analysis was run on the species clustering with the iterative removal of species, first singletons (species with only one individual in the whole data set), doubletons (species with only two individuals in the whole dataset), single core species (species occurring in only one core) and finally, double core species (species only occurring in two cores). Singletons and doubletons both had low sums of square values (0.0006, 0.0028 respectively) and high correlation symmetric rotation values (0.9997 and 0.9986 respectively) in comparison with the single and double species core outputs. As such the single and double core removed datasets were dropped and the singletons and doubletons were then tested with a cluster stability assessment (Henning, 2024). The removal of singletons results in the most stable clusters and therefore the most suitable dataset for the ordination. As such, all ordinations were performed with the singletons removed from the cores. A Hellinger transformation was applied, as it is capable of handling data sets with high abundances and lots of zero values, allowing for a meaningful species composition (Legendre and Gallagher, 2001). This was followed by a beta-diversity Bray-Curtis (Bray and Curtis, 1957) dissimilarity matrix in 'vegan' for the NMDS plot. This was used to compare the composition of similarity between species and stations.

Vials from station KHT 01 and DF 04 (2–5 cm) were dried out post ship-based counting and prior to identification. These vials were included in the abundance-based analysis, as counts were collected on board the ship. However, they were excluded from the ordination analysis, which relies on species richness and species level data, as the presence or removal of a group of unidentified individuals would bias the results, removing the core or core horizon was most appropriate.

Environmental variable data, including near seafloor temperature, salinity, and sediment concentrations of dissolved methane were analysed with the envfit, environmental fitting analysis, which assess the relationship between environmental variables and ordination results. DF 03 depth 2–5 cm, CT 06 depth 0–2 cm, and the whole of CB 07, and RT 13 were removed for the environmental biological analyses, as a result of gaps in the environmental data. As there were fewer data points for this data set after the removal of stations, data were square root transformed followed by a Bray-Curtis dissimilarity matrix (Bray and Curtis, 1957) for the NMDS. Sulfate/Methane Transition (SMT) was determined by identifying the steepest point of concentration change on the plot and using the equation of the line to estimate the sediment depth at which sulfate concentrations reach zero.

2.5 Comparison of South Georgia MUC assemblages with existing higher taxon & polychaete family level data sets

Higher level (class and order) assemblages data collected by MUC from six previous international expeditions were gathered to compare assemblages from other locations in the Southern Ocean to our M134 dataset. Data were taken from the analysis of eight separate cruises: five expeditions during the 1999–2001 FOODBANCS project (Glover et al., 2008); the RV POLARSTERN PS81 expedition to the Antarctic Peninsula of 2013 (Säring et al., 2022, 2021a); the RV POLARSTERN PS96 expedition to the Weddell Sea of 2015/2016 (Säring et al., 2021b, 2022); and the RRS JAMES COOK Cruise JC55 of 2011 (Bell et al., 2016a, 2016b). Combined data table available at Anderson et al. (2025). Locations included the Weddell Sea, Northern Antarctic Peninsula (NAP) and South Georgia. Samples were collected from the shelf at depths ranging from 247 m (JC55, SG) to 1311 m (JC55, Hydrothermal Northern Antarctic Peninsula (HT NAP)). These samples were taken from hydrothermal (HT) and methane (JC55) areas, as well as from regions with a persistent sediment reservoir of labile organic matter due to reduced microbial remineralization

(FOODBANCS), background carbon levels (PS81, PS96), and both ice-free and ice-covered areas (PS96)(Figure 1). All taxa data apart from FOODBANCS were available in the scaled abundances per m^2, so FOODBANCS dataset was also scaled using the code described above (Anderson, 2025). As core horizons were cut differently for each expedition, cores were analysed by 0–5 cm horizons. Tables of taxa were then combined at the lowest possible taxonomic level available, to compare MUC macrofauna assemblages in the Southern Ocean. MUC cores were pooled to singular stations. As the taxonomic levels were higher, abundance data were square root transformed followed by a Bray Curtis dissimilarity matrix.

Only six of the expeditions had data available for polychaetes identified to order and family level. These data came from the JC55 expedition and five FOODBANCS expeditions, allowing for an assemblage comparison within this phylum (combined data table available at Anderson et al., 2025). As these data were to a lower taxonomic level, and cores were not pooled, data were Hellinger transformed (Legendre and Gallagher, 2001), followed by a Bray Curtis dissimilarity matrix.

3 Results

3.1 Environmental variables

Environmental variables were collected during CTD stations at eight stations in seven South Georgia troughs (Figure 1, Table 2). Stations varied in depth from the shallowest at Cumberland East Bay, a large bay on the northern side of the island (CB 07, 136 m) to the deepest at the northern Church Trough (CT 05, 369 m) (Table 2). Near seafloor water temperature had a range of 1.14 °C. The minimum temperature (0.73 °C, CB 08) was recorded within Cumberland Bay, while the highest near seafloor temperature was recorded on the southern part of the continental shelf within the Annenkov Trough - West (1.87 °C, AT-W 11), which was the second deepest location sampled. Near seafloor seawater salinity had a range of 0.49. The minimum and maximum near seafloor water salinities were also recorded at the Cumberland Bay station (33.94, CB 08) and Annenkov Trough - West (34.43, AT-W 11). Concentration of near seafloor seawater dissolved oxygen had a range of 2.94 mLL^{-1}. The minimum dissolved oxygen concentration was 4.12 mLL^{-1} within Annenkov Trough - West (AT-W 11) and there was a 0.49 difference between it and Annenkov Trough - East (AT-E 12). The maximum dissolved oxygen concentration was 7.06 mLL^{-1}(CB 08) within Cumberland Bay.

Surface pore water (i.e., horizon 0 cm) iron (Fe2+) had a maximum concentration of 13.90 mgL^{-1} at Annenkov Trough – East (AT-E 12) (Table 3). Phosphate (PO43-) also reached its maximum concentration at the eastern Annenkov Trough (13.56 $\mu molL^{-1}$). The minimum phosphate concentration was recorded at Cumberland Bay (CB 07) (1.70 $\mu molL^{-1}$), which also had the lowest silicate concentration (38.70 $\mu molL^{-1}$). Maximum concentrations of surface pore water ammonium (11.84 $\mu molL^{-1}$) and sulfate (28.04 $mmolL^{-1}$) sampled were at King Haakon Trough (KHT 01). Chloride had a maximum concentration of 541.40 $mmolL^{-1}$ at the shallower Cumberland Bay station (CB 07), whereas the minimum chloride (534.62 $mmolL^{-1}$) and sulfate (27.62 $mmolL^{-1}$) concentrations were recorded at the Royal Trough stations (RT 13 and RT 14). Dissolved inorganic carbon (DIC) was highest at the deeper, western Church Trough station (CT 05, 3.30 $mmolL^{-1}$) and lowest at the inner Drygalski Fjord (DF 03, 1.77 $mmolL^{-1}$).

The lengths of the MUC cores sampled for methane concentration analysis ranged between 26 cm at Royal Trough (RT 14) and 49 cm at Drygalski Fjord and Cumberland Bay (DF 03, CB 07; Figure 3). Surface pore water methane concentration had a range from 0.28 $\mu molL^{-1}$ at the King Haakon Trough (KHT 01) to 3.11 $\mu molL^{-1}$ at the deeper Church Trough (CT 05). However, most of the locations had surface methane concentration between 0.28 and 0.85 $\mu molL^{-1}$ with the higher of these concentrations found within sediments from the Annenkov Trough - East (AT-E 12). The second lowest methane concentration (0.30 $\mu molL^{-1}$) was found at the Annenkov Trough - West (AT-W 11). The deeper Church Trough (CT 05) was the only station where ikaite crystals were found within the MUC; Church Trough and the Annenkov Trough -West gravity cores also had ikaites in them, at approximately 692 to 696 cm deep at Church Trough, and found at both 290 and 570 cm at the Annenkov Trough - West. The down-core concentration profiles of methane (Figure 3) in the MUC cores varied across the sampled locations, with maximum concentrations at the bottom of the cores ranging from a minimum at the inner Drygalski Fjord (DF 03) 0.6 $\mu molL^{-1}$ to 1267.6 $\mu molL^{-1}$ at the deeper Church Trough station (CT 05). Maximum sulfate concentrations were found at the sediment surface, matching seawater background levels of 28 mmol L^{-1} (e.g., at King Haakon Trough station, KHT 01). In contrast, the lowest pore water concentration was recorded at 30 cm depth in the deep Church Trough core, reaching 4.8 mmol L^{-1}. None of the stations had the Sulfate-Methane Transition (SMT) within the length of the MUC core (Figure 3). Although, the shallowest SMT was located at 37 cm at the deeper Church trough station (CT 05). The King Haakon Trough (KHT 01) had the second shallowest SMT at 115 cm. Royal Trough does not seem to have AOM occurring in the sediments. Hydrogen sulfide was only detected at 3 stations; in very high concentrations at the sediment surface at Church Trough (CT 05), and in lower concentrations at approximately 25–35 cm depth at King Haakon Trough (KHT 01) and the Annenkov Trough - East (AT-E 12) (Supplementary Materials 3).

3.2 Macrofaunal abundance

In total 38 MUC cores from 11 stations (Figure 1, Table 1) were collected for macrofaunal analyses. Overall, 3054 macrofaunal specimens were collected, counted and identified; these belong to a total of 8 phyla, 21 higher taxa and 103 species (Anderson et al., 2025). Based on the taxonomic assessment, the species collected resemble representatives of the known Southern Ocean macrofauna present in soft sediment habitats.

TABLE 3 Concentrations of selected pore water ingredients in shallow sediments (horizons 0 cm and 2 cm below seafloor) collected at MUC stations.

Station	Core Horizon (cm)	Methane (μmol^{-1})	DIC ($mmol^{-1}$)	$Iron^{2+}$ ($mg\ L^{-1}$)	Silicon (μmol^{-1})	Phosphate (μmol^{-1})	Ammonium (μmol^{-1})	Chloride ($mmol^{-1}$)	Sulphate ($mmol^{-1}$)
KHT 01	0	0.28	2.24	0	93.50	4.30	11.84	541.13	28.04
KHT 01	2	0.35	2.71	0.24	306.80	6.84	18.03	543.64	28.42
DF 03	0	0.37	1.77		62.60	4.22	9.48	535.31	27.72
DF 03	2	0.3	2.98	11.20	486.24	81.76	135.27	529.76	27.13
DF 04	0	0.47	2.28	0.00	58.86	7.98	2.49	535.78	27.71
DF 04	2	0.55	2.28	3.38	419.40	37.06	31.51	533.62	27.60
CT 05	0	3.11	3.30	6.02	58.50	3.66	2.386	539.16	27.79
CT 05	2	14.94	3.63	0.07	635.96	40.64	93.51	538.43	26.74
CB 07	0	0.55	2.55	0.00	38.70	1.704	0.00	541.40	28.00
CB 07	2	0.79	2.55	0.12	158.72	0.876	5.49	539.36	28.08
CB 08	0	0.47	2.64	0.01	42.72	1.86	0.00	539.60	27.94
CB 08	2	0.60	2.64	1.64	347.69	6.9275	0.00	539.52	28.00
AT-W 11	0	0.30							
AT-W 11	2	0.79							
AT-E 12	0	0.85	2.50	13.90	76.79	13.56	0.00	539.31	27.78
AT-E 12	2	0.74	3.28	22.32	673.61	163.36	60.01	541.09	27.76
RT 13	0	0.60	2.16		72.55	1.96	0	534.62	27.62
RT 13	2	0.68	2.64	5.02	533.15	15.12	12.57	537.89	27.80
RT 14	0	0.52			65.44	3.17	0	534.62	27.62
RT 14	2	0.47	2.16	2.53	604.07	22.09	17.69	537.89	27.80

DIC, Dissolved Inorganic Carbon. KHT, King Haakon Trough; DF, Drygalski Fjord; CT, Church Trough, CB, Cumberland Bay, AT-W, Annenkov Trough – West; AT-E, Annenkov Trough – East; RB, Royal Bay Trough. NA, Blank cells not available as these samples were not collected.

3.2.1 Species diversity

The highest species richness was observed at the Annenkov Trough - West station with 51 species (AT-W 11) and was lowest at Church Trough and Cumberland Bay (station CT 06, CB 07 and CB 08), which all had 19 species (Table 4). Although Annenkov Trough - West (AT-W 11) was the most highly sampled station with five cores, richness was not solely determined by sampling effort but also by environmental and geochemical factors, as seen by the species accumulation curve (Supplementary Materials 2). Pielou's evenness indicated that the deeper Cumberland Bay (CB 08, 0.89) and deeper Church Trough (CT 05, 0.88) were the two most even stations while the inner Drygalski Fjord (DF 03, 0.48) was the least even (Table 4). The Shannon-Wiener Diversity Index, ranged from values of 1.48 (inner Drygalski Fjord, DF 03) to 3.11 (Royal Trough, RT 14). The Royal Trough station RT 14 therefore has a more diverse and evenly distributed assemblage. The inner Drygalski Fjord (DF 03) has a comparatively lower species diversity or uneven distribution. The inverse Simpson Diversity also has the inner Drygalski Fjord (DF 03) as the least diverse station (2.25) and both the Royal Trough (RT 14) and deeper Church Trough (CT 05) as the most diverse stations (16.46, 15.86 respectively). Therefore both measures for diversity are in agreement that Royal Trough (RT 14) is the most diverse station, with the inner Drygalski Fjord station (DF 03) having the lowest diversity and evenness.

3.2.2 Assemblage composition

Arthropoda were the most species rich phylum (50 species), followed by Annelida (32 species) and then Mollusca (11 species) (Table 5). At the class level, the Malacostraca (38 species from Amphipoda (15 spp), Cumacea (3 spp), Decapoda (1 spp), Isopoda (12 spp), Mysida (1 spp) and Tanaidacea (6 spp)) are the most species rich, followed by the Polychaeta (31 species)(Table 5). Holothurida had a low diversity and abundance and only one specimen of Bryozoa was collected.

Annelida were the most abundant phylum (mean abundance 4785.3 ± 1753.54 m^{-2}) and were present at every station. Lowest polychaete abundance (909.5 ± 126.3 m^{-2}) was at one of the Cumberland Bay stations (CB 08) and the highest at Annenkov Trough – West (3023.2 ± 2898.8 m^{-2}). Nematoda (1207.6 ± 1014.7 m^{-2}) and Arthropoda (1166.1 ± 434.08 m^{-2}) were the next most abundant phyla. Nematodes were present at all stations apart from the shallower Cumberland Bay station (CB 07). Maximum nematode

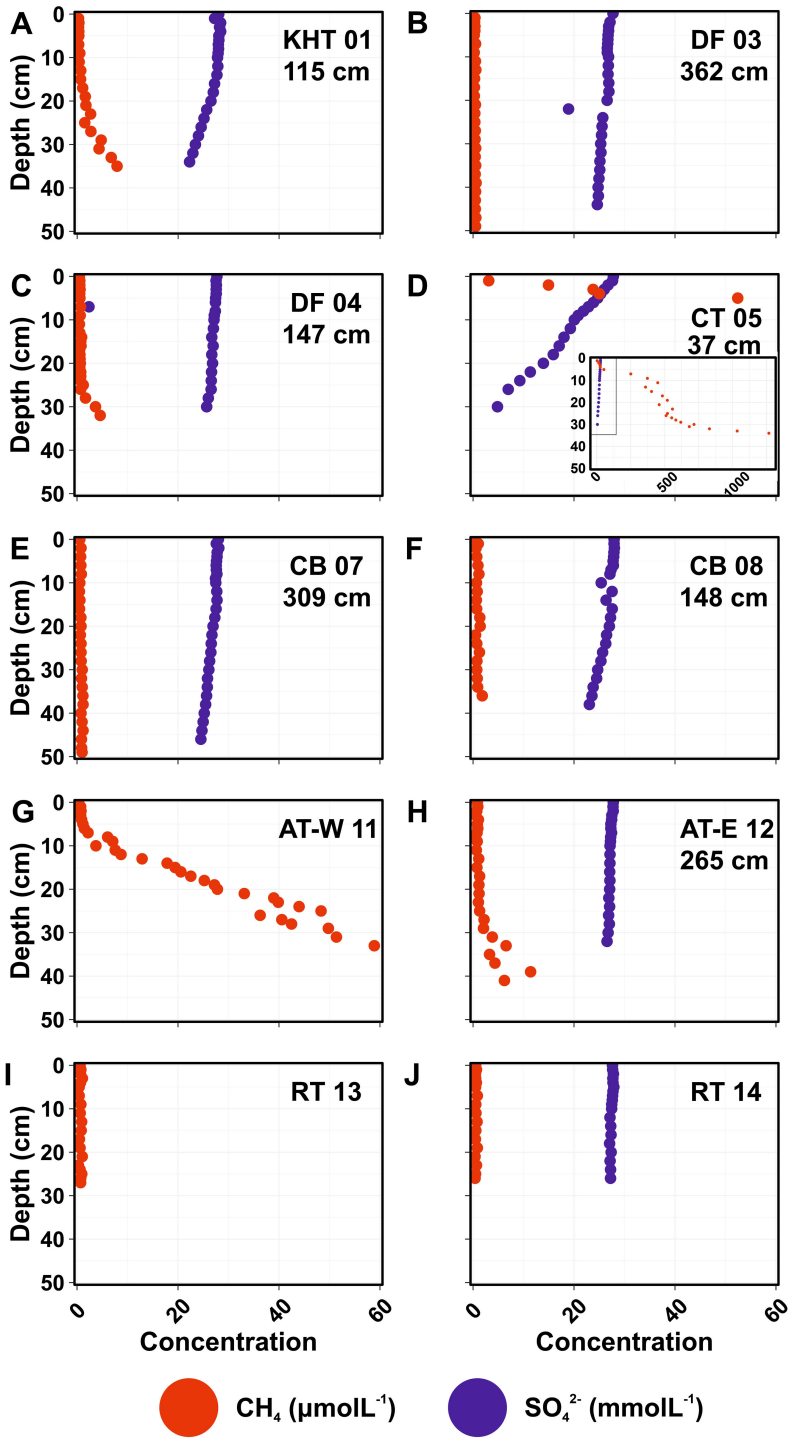

FIGURE 3
Pore-water concentration profiles of the methane (red) and sulfate (blue) in South Georgia sediments, with approximate Sulfate-Methane Transition depth in cm. **(A)** KHT, King Haakon Trough; **(B, C)** DF, Drygalski Fjord; **(D)** CT, Church Trough; **(E, F)** CB, Cumberland Bay; **(G)** AT-W, Annenkov Trough – West; **(H)** AT-E Annenkov Trough – East; **(I, J)** RT, Royal Trough.

abundance (4692.8 ± 2658 m^{-2}) was at the inner Drygalski Fjord (DF 03) and minimum abundance (18.2 ± 18.2 m^{-2}) was at one of the Cumberland Bay stations (CB 08). A minimum of one Arthropoda taxa is present at every station, with only one at Cumberland Bay station (CB 07) but a maximum of seven of the Arthropoda taxa were represented at three stations, the inner Drygalski Fjord (DF 03), and both of the stations within the Annenkov Trough - West and -East (AT-W 11 and AT-E 12). The most abundant Arthropoda taxa were the tanaids (251.1 ± 280.7 m^{-2}) and the least abundant were the decapods and mysids (1.7 ± 5.5 m^{-2}). The highest overall abundance at a station of any

10.3389/fmars.2025.1589660

TABLE 4 Number of cores collected per station (No. cores) and diversity indices by station.

Station	No. Cores	Ave Abun (m^{-2}) ± SE	Species Richness	Pielou Evenness	Shannon-Wiener Diversity	Inverse Simpson Diversity
KHT 01	1	28903	27	0.75	2.47	6.40
DF 03	4	12531 ± 6523	22	0.48	1.48	2.25
DF 04	3	27389 ± 1873	36	0.66	2.36	7.52
CT 05	4	6023 ± 1353	32	0.88	3.04	15.86
CT 06	2	10250 ± 5157	19	0.72	2.12	5.32
CB 07	3	3820 ± 1901	19	0.76	2.25	5.93
CB 08	4	3303 ± 785	19	0.89	2.61	11.30
AT-W 11	5	30300 ± 4025	51	0.60	2.35	4.52
AT-E 12	4	18816 ± 3479	29	0.63	2.14	4.90
RT 13	4	6582 ± 1717	31	0.82	2.82	11.14
RT 14	4	6826 ± 757	38	0.86	3.11	16.46

Ave abun, Average abundance; SE, Standard error; KHT, King Haakon Trough; DF, Drygalski Fjord; CT, Church Trough; CB, Cumberland Bay; AT-W, Annenkov Trough – West; AT-sE, Annenkov Trough – East; RT, Royal Trough.

Arthropoda taxa, was the Amphipoda (1004.4 ± 238 m^{-2}) at Annenkov Trough - West (AT-W 11). Mean molluscan abundance was 461.6 ± 255.55 m^{-2} with a maximum bivalve abundance of 140.9 ± 688.5 m^{-2} at the outer Drygalski Fjord (DF 04) and a minimum bivalve abundance of 31.8 ± 31.8 m^{-2} at Annenkov Trough -East (AT-E 12). Bivalves were present at all stations, apart from the inner Drygalski Fjord (DF 03). Gastropods are only present at one of the Church Trough stations (CT 05), one of the Cumberland Bay stations (CB 08) and both Annenkov Trough stations (AT- W 11, AT-E 12) and Royal Trough (RT 13, RT 14).

Macrofauna was absent in the 2–5 cm horizon of MUC cores from the inner Drygalski Fjord (DF 03-10), Church Trough stations (CT 05-08, CT 06-02), Cumberland Bay (CB 07-04, CB 08-02), and Annenkov Trough (AT-W 11-12). As the Church Trough (CT 06-02) core is the only core from the station CT 06, it is therefore absent from the 2–5 cm core horizon abundance plot. Species assemblages vary across core horizons (0–2 cm and 2–5 cm). 0–2 cm core horizons have a higher richness of phyla and species with 12–47 species versus the 2–5 cm core horizons with 7–23 species (Figures 4A, C). At the shallower Church Trough (CT 06) all 19 species at the station were found in the top 0–2 cm horizon. At the deeper Annenkov Trough station (AT-W 11) 47 of the 52 species were found in the 0–2 cm horizon. In comparison, in the 2–5 cm core horizon (Figures 4B, D) all but two stations have over 50% of their assemblages made up of Polychaeta. The deeper Annenkov Trough station (AT-W 11) had the highest abundance per m^{-2} (a mean of 30,300 ± 4025 m^{-2}, Table 4 and Table 5). This abundance was dominated by Annelida (13,062 ± 2897.5 m^{-2}) and Arthropoda (3,103.0 ± 452.8 m^{-2})(Figure 4). King Haakon Trough (KHT 01, 28,903 m^{-2}) and outer Drygalski Fjord (DF 04, 27,389 ± 1,873 m^{-2}) stations also had high abundances with Annelida dominating the assemblage for them both (8,148.7 ± 1,655.2 m^{-2} and 9,844 ± 1,341.6 m^{-2} respectively). The King Haakon Trough (KHT 01) station was dominated by Arthropoda (2,928.4 ± 1,115.8 m^{-2}) and Nematoda (2228.2 ± 63.7 m^{-2}). Along with the Annelida, a large proportion of the outer Drygalski Fjord station (DF 04) assemblage was dominated by Mollusca (2,140.9 ± 688.5 m^{-2}). The deeper Cumberland Bay station (CB 08) and the deeper Church Trough station (CT 05) had the lowest abundances (3,303 ± 785 m^{-2} and 6023 ± 1353 m^{-2} respectively). The deeper Church Trough station (CT 05) was dominated by Annelida (1,548.1 ± 526.7 m^{-2}) and Arthropoda (1,168.1 ± 194.8 m^{-2}).

Annelida consistently dominated the station assemblages, particularly at the King Haakon Trough station (KHT 01, 78%), outer Drygalski Fjord (DF 04, 69%), and shallower Church Trough (CT 06, 67%) (Figures 4A, B, Table 5). The lowest relative Annelida abundance was at the inner Drygalski Fjord station (DF 03) making up 22% of the assemblage while Nematoda dominated the assemblage at this station (62%).

3.3 Macrofaunal assemblage and environment at South Georgia

The NMDS ordination based on the observations of macrofauna present in the cores indicated that there were differences in assemblages between 0–2 cm horizon and the 2–5 cm horizon (Figure 5A). The major trend was observed along the NMDS axis 1 where the majority of samples that were represented by the 0–2 cm core horizon have NMDS1 values less than 0 (Figure 5A). Within the ordination it was difficult to decipher a clear pattern in the stations even considering those that were collected from a similar trough. For example, the samples from the Annenkov Trough - West station in the 0–2 cm horizon grouped together, however those from the Annenkov Trough - East station were found closer to the Royal Bay (RB 13 and RB14) which was to the east of South Georgia. This is likely as a result of Annenkov Trough - West (AT-W 11), having the highest abundances of the widespread Maldanidae species (species 8,

TABLE 5 Normalised mean abundances (m^{-2}) with standard error (Abun) and species richness (SR) by phylum and taxon per station.

Phylum	Taxon	Abun/SR	Mean Abun/Total SR	KHT 01	DF 03	DF 04	CT 05	CT 06	CB 07	CB 08	AT-W 11	AT-E 12	RT 13	RT 14
Arthropoda	Amphipoda	Abun	302.4 ± 157	827.6 ± 318.3	86.9 ± 57.1	466.9 ± 251.8	301.1 ± 119	0 ± 0	0 ± 0	127.3 ± 127.3	1004.4 ± 238	235.2 ± 73	105.1 ± 67.9	171.5 ± 78.3
		SR	15	4	2	6	3	0	0	2	11	4	3	4
Arthropoda	Copepoda cala.	Abun	38.4 ± 58.9	0 ± 0	151.6 ± 151.6	127.3 ± 104	0 ± 0	0 ± 0	0 ± 0	0 ± 0	0 ± 0	143.2 ± 65.6	0 ± 0	0 ± 0
		SR	2	0	1	1	0	0	0	0	0	2	0	0
Arthropoda	Copepoda harp.	Abun	128.8 ± 160.4	445.6 ± 445.6	188 ± 102.7	0 ± 0	18.2 ± 18.2	0 ± 0	0 ± 0	0 ± 0	0 ± 0	567.7 ± 247.6	137.4 ± 101.5	60.1 ± 44.8
		SR	5	3	4	0	1	0	0	0	0	3	2	2
Arthropoda	Cumacea	Abun	42.5 ± 42	0 ± 0	0 ± 0	0 ± 0	68.7 ± 50.8	63.7 ± 63.7	0 ± 0	18.2 ± 18.2	237.4 ± 102.3	63.7 ± 41.7	0 ± 0	15.9 ± 15.9
		SR	3	0	0	0	1	1	0	1	2	2	0	1
Arthropoda	Decapoda	Abun	1.7 ± 5.5	0 ± 0	18.2 ± 18.2	0 ± 0	0 ± 0	0 ± 0	0 ± 0	0 ± 0	0 ± 0	0 ± 0	0 ± 0	0 ± 0
		SR	1	0	1	0	0	0	0	0	0	0	0	0
Arthropoda	Isopoda	Abun	212.2 ± 139.9	63.7 ± 63.7	390.1 ± 237.9	212.2 ± 163.3	254.6 ± 107.6	191 ± 63.7	152.8 ± 123.4	151.6 ± 151.6	292.4 ± 190.5	367.8 ± 172.4	54.6 ± 54.6	203.4 ± 70.8
		SR	12	1	1	3	2	2	2	1	5	2	2	6
Arthropoda	Mysida	Abun	1.7 ± 5.5	0 ± 0	18.2 ± 18.2	0 ± 0	0 ± 0	0 ± 0	0 ± 0	0 ± 0	0 ± 0	0 ± 0	0 ± 0	0 ± 0
		SR	1	0	1	0	0	0	0	0	0	0	0	0
Arthropoda	Ostracoda	Abun	32.5 ± 45.4	0 ± 0	50.5 ± 50.5	21.2 ± 21.2	54.6 ± 37.9	0 ± 0	0 ± 0	177.8 ± 128.9	53.4 ± 40.1	0 ± 0	0 ± 0	0 ± 0
		SR	4	0	1	1	3	0	0	1	2	0	0	0
Arthropoda	Pantopoda	Abun	154.8 ± 179.8	636.6 ± 509.3	0 ± 0	42.4 ± 26.8	0 ± 0	0 ± 0	0 ± 0	0 ± 0	808 ± 290.9	215.7 ± 104.7	0 ± 0	0 ± 0
		SR	1	1	0	1	0	0	0	0	1	1	0	0
Arthropoda	Tanaidacea	Abun	251.1 ± 280.7	954.9 ± 827.6	0 ± 0	21.2 ± 21.2	470.9 ± 134.1	0 ± 0	0 ± 0	0 ± 0	707.4 ± 313.6	15.9 ± 15.9	416.3 ± 243.1	175.1 ± 75.9
		SR	6	2	0	1	3	0	0	0	2	1	5	3
Annelida	Clitellata	Abun	3.6 ± 11.8	0 ± 0	0 ± 0	0 ± 0	0 ± 0	0 ± 0	0 ± 0	0 ± 0	39.3 ± 39.3	0 ± 0	0 ± 0	0 ± 0
		SR	1	0	0	0	0	0	0	0	1	0	0	0

(Continued)

10.3389/fmars.2025.1589660

TABLE 5 Continued

Phylum	Taxon	Abun/ SR	Mean Abun/ Total SR	KHT 01	DF 03	DF 04	CT 05	CT 06	CB 07	CB 08	AT-W 11	AT-E 12	RT 13	RT 14
Annelida	Polychaeta	Abun	4781.7 ± 1753.5	8148.7 ± 1655.2	1509.7 ± 694.3	9844 ± 1341.6	1548.1 ± 526.7	8085.1 ± 4138	1850.4 ± 822.5	909.5 ± 126.3	13023.2 ± 2898.8	3929.4 ± 1427	1685.5 ± 384.9	2065.5 ± 345.5
		SR	31	10	8	16	11	12	14	9	17	10	12	17
Bryozoa	Bryozoa	Abun	5.8 ± 19.2	63.7 ± 63.7	0 ± 0	0 ± 0	0 ± 0	0 ± 0	0 ± 0	0 ± 0	0 ± 0	0 ± 0	0 ± 0	0 ± 0
		SR	1	1	0	0	0	0	0	0	0	0	0	0
Echinodermata	Holothuroida	Abun	47.6 ± 153.6	509.3 ± 509.3	0 ± 0	0 ± 0	0 ± 0	0 ± 0	0 ± 0	0 ± 0	14.1 ± 14.1	0 ± 0	0 ± 0	0 ± 0
		SR	1	1	0	0	0	0	0	0	1	0	0	0
Echinodermata	Ophiuroidea	Abun	29.8 ± 60.9	0 ± 0	0 ± 0	0 ± 0	54.6 ± 37.9	191 ± 191	0 ± 0	0 ± 0	81.7 ± 54.1	0 ± 0	0 ± 0	0 ± 0
		SR	2	0	0	0	1	1	0	0	1	0	0	0
Mollusca	Bivalvia	Abun	438.7 ± 251	573 ± 318.3	0 ± 0	2140.9 ± 688.5	177.8 ± 94.3	318.3 ± 191	121.7 ± 76.1	297.1 ± 115.3	473.1 ± 159	31.8 ± 31.8	373.9 ± 123.5	318.3 ± 107.6
		SR	5	3	0	3	2	1	2	1	3	1	2	2
Mollusca	Gastropoda	Abun	22.9 ± 48	0 ± 0	0 ± 0	0 ± 0	151.6 ± 151.6	0 ± 0	0 ± 0	36.4 ± 36.4	14.1 ± 14.1	15.9 ± 15.9	18.2 ± 18.2	15.9 ± 15.9
		SR	5	0	0	0	1	0	0	2	1	1	1	1
Nemertea	Nemertini	Abun	144.1 ± 227.2	0 ± 0	0 ± 0	21.2 ± 21.2	18.2 ± 18.2	509.3 ± 509.3	166.9 ± 137.3	151.6 ± 105.2	14.1 ± 14.1	486.3 ± 486.3	202.1 ± 202.1	15.9 ± 15.9
		SR	2	0	0	1	1	1	1	1	1	1	2	1
Nematoda	Nematoda	Abun	1207.6 ± 1014.7	2228.2 ± 63.7	4692.8 ± 2658	754.5 ± 261.1	200.1 ± 114.1	891.3 ± 509.3	0 ± 0	18.2 ± 18.2	42.4 ± 21.2	3335.2 ± 1935.3	749.8 ± 392	371.4 ± 127.8
		SR	1	1	1	1	1	1	0	1	1	1	1	1
Sipunculida	Sipunculida	Abun	8.4 ± 12	0 ± 0	0 ± 0	42.4 ± 26.8	18.2 ± 18.2	0 ± 0	0 ± 0	0 ± 0	14.1 ± 14.1	0 ± 0	18.2 ± 18.2	0 ± 0
		SR	2	0	0	2	1	0	0	0	1	0	1	0
Indet	Indet	Abun	15.8 ± 23.8	0 ± 0	54.6 ± 54.6	0 ± 0	105.1 ± 55.4	0 ± 0	0 ± 0	0 ± 0	14.1 ± 14.1	0 ± 0	0 ± 0	0 ± 0
		SR	2	0	2	0	1	0	0	0	1	0	0	0

KHT, King Haakon Trough; DF, Drygalski Fjord; CT, Church Trough; CB, Cumberland Bay; AT-W, Annenkov Trough – West; AT-E, Annenkov Trough - East, RT, Royal Trough.

10.3389/fmars.2025.1589660

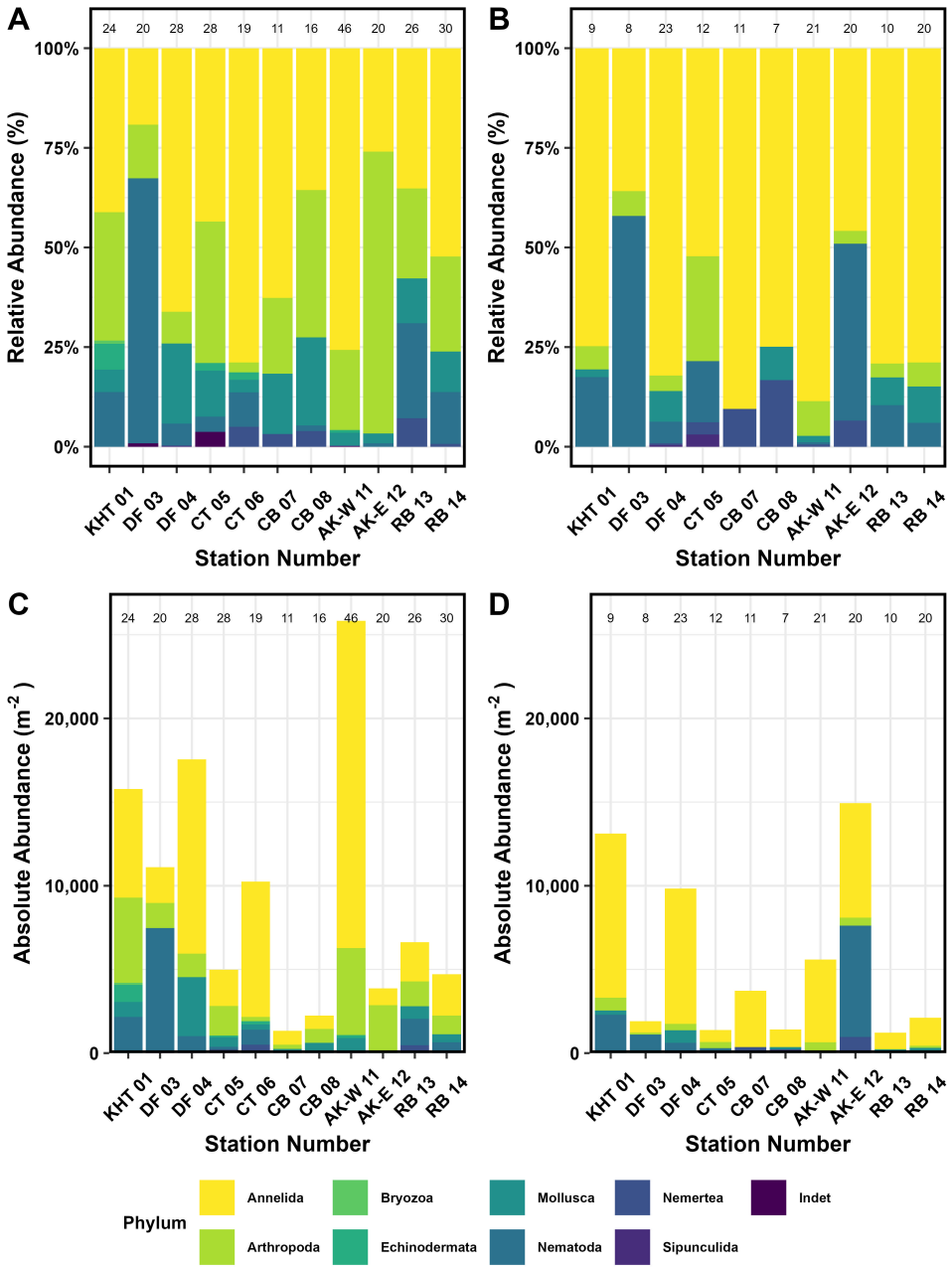

FIGURE 4
Species abundance by phyla. **(A, B)** Relative abundance of phyla per station, with species richness noted at the top of each bar. **(C, D)** Absolute abundance (m^{-2}) of phyla per station, with species richness noted at the top of each bar. **(A)** and **(C)** are from the 0–2 cm core horizon, and **(B)** and **(D)** from the 2–5 cm horizon. KHT, King Haakon Trough; DF, Drygalski Fjord; CT, Church Trough; CB, Cumberland Bay; AT-W, Annenkov Trough - West; AT-E, Annenkov Trough - East; RB, Royal Bay Trough.

9, Figure 5 and Supplementary Materials 5). Ampharetidae sp. 2 (3, Figure 5 and Supplementary Materials 5), Lumbrineridae (7, Figure 5 and Supplementary Materials 5), and Opheliidae (12, Figure 5 and Supplementary Materials 5) all have their highest abundances at the Annenkov Trough - West (AT-W 11). Whereas the Capetillidae (4, Figure 5 and Supplementary Materials 5) were present in higher abundances in the Annenkov Trough - East (AT-E 12) and Royal Bay (RB 13). Even at specific stations there was variability in the spread of data points. For example, the samples 0–2 cm horizon from the Annenkov Trough - West location grouped together in the NMDS while those from Cumberland Bay were much more dispersed (CB 07 and CB 08). In the case of Cumberland Bay the 0–2 cm and 2–5 cm horizon depths were separated by a much larger distance on the ordination in comparison to the two depth horizons from the Annenkov Trough - West; this indicated that there could be considerable within-station variability in the assemblage. Terebelliformia (27, Figure 5 and Supplementary Materials 5) and Trichobranchidae (sp. 1, 29, Figure 5 and Supplementary Materials 5) were only in the 2–5 cm core horizons, and Cirratulidae (sp. 1, 5, Figure 5 and Supplementary Materials 5) abundances were very

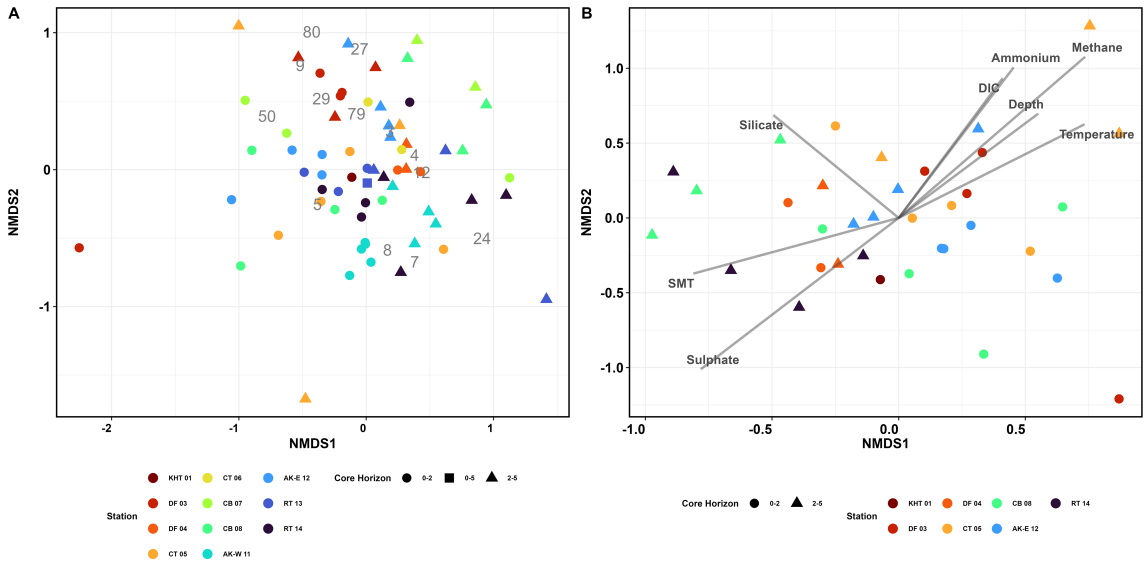

FIGURE 5
NMDS of stations as **(A)** Separate cores and core horizons 0-2 and 2-5 cm, with one station as 0-5 cm corresponding species numbers are in the Supplementary Materials 5. Singletons removed. Stress = 0.196. and **(B)** stations and core horizons as plotted against environmental data. Singletons removed. Stress = 0.181.

variable within both the cores and core horizons in the Cumberland Bay stations.

When the vectors of variable contribution were overlaid on those stations with comparable data, it was possible to begin to resolve what was potentially driving some of the variability among the stations (Figure 5B). The vertical dimensions of the ordination (NMDS axis 2) were clearly associated with temperature, methane, DIC and ammonium while SMT and sulfate were negatively associated to these environmental variables. The environmental variables including methane and sulfate had a significant influence

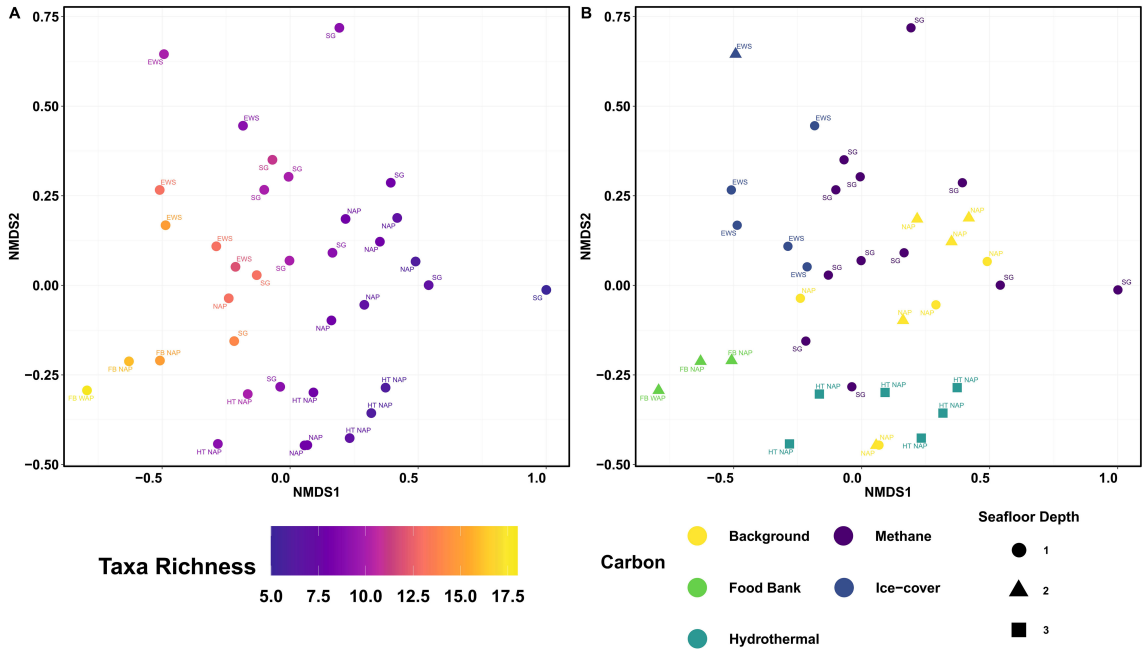

FIGURE 6
NMDS of MUC assemblage data from nine expeditions in the western portion of the Southern Ocean. **(A)** Taxa richness. **(B)** Seafloor depth is split into 1. 0–500 m, 2. 500–1000 m and 3. 1000+ m, and colours by the carbon source of the area. Food Bank is in reference to Glover et al. (2008), finding year round sediment food bank in the NAP. Ice cover is defined from Säring et al. (2022) where ice-cover amount, duration, and fluctuation were obtained for the preceding nine years. EWS, Eastern Weddell Sea; HT NAP, Hydrothermal Northern Antarctic Peninsula; NAP, Northern Antarctic Peninsula; SG, South Georgia; FB NAP, FOODBANCS Northern Antarctic Peninsula. Stress = 0.179.

on the benthic assemblage structure (envfit: $p<0.001$), as did ammonium (envfit: $p<0.01$). Temperature, DIC, silicate and SMT depth show some influence (envfit: $p<0.05$). Surface porewater methane had the highest concentrations recorded at Church Trough which were some of the most extreme points on vertical axes. Ammonium was also elevated in the Drygalski Fjord, King Haakon Trough and Church Trough stations which were mainly those with positive NMDS axis 2 scores. Salinity, oxygen, phosphate and chloride do not show significant influence on the assemblage.

3.4 Macrofaunal assemblage in soft sediment habitats across the Southern Ocean

The assemblages from stations sampled in this study at South Georgia, were compared to previous studies in the Southern Ocean which investigated soft-sediment assemblages influenced by methane seeps, hydrothermal activity, high organic-carbon content, or sediments across different ice cover regimes and therefore different amounts of particulate organic matter input from surface waters but not influenced by chemosynthetic primary production (i.e. "background" sediments). 11 MUC cores from this study were analysed alongside 29 MUC cores from previous studies (Figure 1, Table available at Anderson et al., 2025).

Abundances ranged from 1,594 m^{-2} in the ice-covered Eastern Weddell Sea (EWS) to 35,142 m^{-2} at the South Georgia Ice Fjord Trough (SG IFT) (Table available at Anderson et al., 2025). Small variability in abundances between stations was observed at the Hydrothermal Northern Antarctic Peninsula (HT NAP, range: 4,648 m^{-2}), Eastern Weddell Sea (EWS, range: 4,841 m^{-2}), South Georgia Ice Fjord Trough (SG IFT, range: 9,740 m^{-2}), and FOODBANCS Northern Antarctic Peninsula (FB NAP, range: 5,434 m^{-2}). In contrast, the South Georgia and Northern Antarctic Peninsula (NAP) stations showed greater variability than the other stations, with abundance ranges of 26,997 m^{-2} and 26,582 m^{-2}, respectively. The Hydrothermal Northern Antarctic Peninsula (HT NAP) and Eastern Weddell Sea (EWS) had the lowest abundances of all stations (HT NAP (1,826 - 6,474 m^{-2}) and EWS (1,594 - 6,435 m^{-2})). The Northern Antarctic Peninsula station abundances ranged from 4,038 to 30,620 m^{-2}, similar to the methane-flux influence stations in South Georgia 3,303 - 30,300 m^{-2}.

The NMDS ordination revealed spatial patterns in macrofaunal composition across the stations (Figure 6). Taxa richness decreased along the NMDS axis 1 (Figure 6A). The persistent labile organic matter in the sediment FOODBANCS Northern Antarctic Peninsula stations have the highest species richness and along with some of the Eastern Weddell Sea and South Georgia stations have NMDS1 values less than 0. To an extent, depth appears to structure the NMDS axis 2, with the deepest stations (e.g., Hydrothermal Northern Antarctic Peninsula) with an NMDS2 value less than 0, mid-depth stations (517–757 m) from FOODBANCS Northern Antarctic Peninsula and Northern Antarctic Peninsula clustered centrally (NMDS2 approx. 0), and the shallowest stations (136–482 m) from the Eastern Weddell Sea with an NMDS2 value greater than 0 (Figure 6B). Some clustering by dominating organic-carbon source was evident, notably, most South Georgia stations aligned more closely with background and ice-covered stations rather than hydrothermal (Hydrothermal Northern Antarctic Peninsula) or persistent labile organic matter in the sediment (FOODBANCS Northern Antarctic Peninsula) environments, suggesting potential similarities in environmental conditions and faunal composition. The exceptions to this are the Ice Fjord Trough and Annenkov Trough (West) station grouping near the hydrothermal and FOODBANCS stations, suggesting the presence of higher organic-carbon at these two South Georgia stations. The three most influential taxa contributing to the observed patterns were Annelida (49.22%), Bivalvia (63.24%), and Nematoda (75.10%).

3.4.1 Polychaete assemblage structure in the Southern Ocean

A total of 52 polychaete taxa were identified from 51 cores collected across seven expeditions (M134, JR55, and FOODBANCS) and four environmental groups: South Georgia methane seeps (SG M134), Ice Fjord Trough (SG JR55), Hook Ridge hydrothermal vents in the Northern Antarctic Peninsula (HT NAP), and the persistent labile organic matter in the sediment stations from FOODBANCS Northern Antarctic Peninsula (FB NAP) (combined data table available at Anderson et al., 2025). Both South Georgia assemblages (from this study, and the Ice Fjord Trough JR55) sat distinct from the FOODBANCS and hydrothermal vent Northern Antarctic Peninsula stations. Notably, taxa from the families Terebellidae, Cirratulidae and Orbiniidae were in the top contributors across multiple comparisons. Between the two sets of South Georgia samples, it was the families Cirratulidae (11.01%), Hesionidae (10.14%) and Orbiniidae (15.6%) which collectively accounted for 36.75% of the dissimilarity observed, suggesting some local environmental differences between the Ice Fjord Trough (IFT) and the rest of the South Georgia shelf samples. The polychaete assemblages from the Annenkov Trough - West cores exhibited low variability, as evidenced by their close clustering in the NMDS ordination (Supplementary Materials 6). This grouping is primarily driven by the dominance of Maldanidae. Notably, the assemblages from Annenkov Trough - West (AT-W 11) show greater similarity to those of the hydrothermal stations in the Northern Antarctic Peninsula (HT NAP) than to those from the Ice Fjord Trough (IFT). In contrast, the polychaete assemblages from Church Trough display greater variability, where several cores cluster centrally within the South Georgia M134 assemblage, where Orbiniidae and Capitellidae are key taxa.

4 Discussion

This study represents the first circum-island shelf investigation of macrobenthic assemblages in the methane seeps around the South Georgia shelf. Seven shelf troughs around the island were investigated to assess diversity, richness, assemblage composition,

and the environmental and geochemical drivers shaping these assemblages. Macrofaunal abundance and species richness was highest at the second deepest station, the Annenkov Trough - West (AT-W 11). Annelida were the most abundant phylum (mean abundance 4785.3 ± 1753.54 m^{-2}) and were present at every station. The environmental variables including methane and sulfate had a significant influence on the benthic assemblage structure; it was difficult to decipher a clear pattern in the stations even considering those that were collected from the same trough. Many stations had variability in their core assemblages. We also compared our results to datasets from other Southern Ocean environments, ranging from "background" organic-carbon levels (stations with ice cover ranging from none to seasonal - Northern Antarctic Peninsula, NAP), to areas with persistent labile organic matter within the sediment (FOODBANCS Northern Antarctic Peninsula, FB NAP), ice-covered regions (high cover and constant - Eastern Weddell Sea, EWS), as well as areas with sediment-hosted hydrothermal influence (HT NAP) and a previous study of methane seeps in the Ice Fjord Trough (IFT) on the South Georgia shelf. Species richness and depth structured the groupings of Southern Ocean assemblages. The observed clustering based on ecosystems resulted in most South Georgia stations aligning more closely with background and ice-covered stations rather than hydrothermal stations or stations with sediments with persistent labile organic matter. The polychaete assemblages from the Annenkov Trough - West cores exhibited low variability, primarily driven by the dominance of Maldanidae. Notably, the assemblages from Annenkov Trough - West (AT-W 11) show greater similarity to those of the hydrothermal stations in the Northern Antarctic Peninsula (HT NAP) than to those from the South Georgia Ice Fjord Trough (IFT). In contrast, the polychaete assemblages from Church Trough (CT 05, the deepest and highest methane-flux influenced station) display greater variability.

4.1 Macrofaunal abundance patterns in the South Georgia methane seeps

The distribution of faunal abundances at methane seeps is influenced by a range of interrelated factors, including the depth of the sulfate/methane transition (SMT), the presence of hydrogen sulfide, and spatial variability in environmental conditions such as sediment composition, fluid flow rates, and gas orifice locations (De Beer et al., 2006; Fischer et al., 2012; Lichtschlag et al., 2010; Niemann et al., 2009; Sahling et al., 2002). However, in our South Georgia study, the SMT depth alone is not a reliable predictor of faunal abundances. For instance, despite having the deepest SMT (14,350 cm) of the study, the Royal Bay Trough (RT 14) had a faunal abundance of 6,826 ± 757 m^{-2}, which was very similar to the Church Trough station (CT 05), with the shallowest SMT of the study (37 cm), which had an abundance of 6,023 ± 1,353 m^{-2}. This suggests that other factors beyond SMT depth play a significant role in determining faunal distribution. At the Makran convergent continental margin, the combination of sulfate flux, depth of sulfide release, and the depth of complete sulfide consumption influences the colonisation of seeps by thiotrophic and chemosynthetic assemblages (Fischer et al., 2012). Each of these geochemical components individually is insufficient to fully describe the environment and its effects on faunal distribution (Wallmann et al., 1997). This is likely because sulfide fluxes and concentrations measured in the sediment do not fully account for hydrogen sulfide production, which is influenced by factors such as sulfide oxidisers, inorganic precipitation with reduced iron, or oxidation with iron hydroxides (Taillefert et al., 2017). Iron reduction, dominates at stations such as Cumberland Bay (CB 07, CB 08), Drygalski Fjord (DF 03, DF 04), and Annenkov Trough (AT-W 11, AT-12 E) (Schnakenberg et al., 2021; Wunder et al., 2021), and these stations exhibit higher faunal abundances compared to the sulfate-reduction dominated Church Trough (CT 05).

Hydrogen sulfide, a byproduct of sulfate-coupled anaerobic methane oxidation (AOM) (Fischer et al., 2012), was detected in the sediments at only three of the 11 stations: at 25 cm depth in King Haakon Trough (KHT 01, SMT 115 cm), and in the western branch of Annenkov Trough (AT-W 11, SMT unknown), and in surface sediments at the Church Trough station (CT 05, SMT 37 cm). The high faunal abundances at the 25 cm depth hydrogen sulfide-influenced stations of King Haakon Trough (28,903 m^{-2}) and Annenkov Trough (30,300 ± 4,025 m^{-2}) suggest an elevated supply of free-living microbial food sources, likely driven by bacterial production utilising hydrogen sulfide (Levin et al., 2010). The higher abundances at the King Haakon and Annenkov Trough stations is similar to findings from cold seeps in the Congo, where the highest macrofaunal densities were observed under "medium" sulfidic conditions (Olu et al., 2017). In the "medium" sulfidic areas, microbial mats were smaller and thinner than those at the Håkon Mosby Mud Volcano, and sulfide concentrations were one or two orders of magnitude lower than those reported from methane seeps along the Northeastern Pacific margin (De Beer et al., 2006; Levin et al., 2003; Sahling et al., 2002). Since sulfide concentrations influence both microbial mat development and the macrofaunal communities that rely on them, the intermediate sulfidic conditions at the King Haakon and Annenkov Trough stations may provide an environment that supports higher macrofaunal abundances by balancing sulfide toxicity and resource availability. In contrast, lower faunal abundances (6,023 ± 1,353 m^{-2}) were found in the Church Trough (CT 05) station where hydrogen sulfide is found in the surface sediments. The low abundance at Church Trough (CT 05) is similar to the Håkon Mosby Mud Volcano, where high surface sulfide concentrations can be toxic to many benthic taxa, and where high fluid flow rates may limit macrofaunal densities (Portail et al., 2015). The high sulfate and methane concentrations at Church Trough result in a sulfate-reduction dominated environment, leading to elevated hydrogen sulfide levels at the sediment surface that likely limit faunal abundance at this station. Whilst this disagrees with the conceptual model of abundance with proximity to hydrothermally active sites (Bernardino et al., 2012), it supports the pattern observed in Bell et al. (2016b), whereby abundance increases and subsequently decreases with increasing hydrothermal influence; the higher methane- and sulfate-flux at

King Haakon Trough and the Annenkov Trough - West, results in higher abundances than in other stations, with lower abundances at the highest flux station of Church Trough.

Faunal abundance and species composition vary within individual stations, with differences observed across multiple cores collected from the same 1x1 m MUC area. A single 6 cm core represents only 28.3 cm^2 (1/353rd of total MUC area), while a 10 cm core represents 78.5 cm^2 (1/127th of total MUC area), both are a fraction of the MUC's 1 m^2 footprint. Within-MUC variability on macrofauna (the sizes range from 500 µm to 5 cm) suggests small-scale habitat heterogeneity influencing assemblage over the scale of tens of centimetres. This small scale heterogeneity is important for understanding assemblage differences within a single MUC sample. Small-scale environment factors, such as methane flux variability, can vary by several orders of magnitude over only a few meters (Torres et al., 2002) and bacterial mat distribution (as a result of geochemical transitions and localised chemotones), likely creates distinct microhabitats between MUC cores (Ashford et al., 2021b; Levin, 1992; Levin et al., 2016). The South Georgia seeps, characterised by orifices and variable bacterial mat coverage (Figure 2), reflect the complexity of physical, geochemical, and biological processes in the sediments on the shelf, and the potential for geochemical microhabitats therefore support differing biological assemblages. These microhabitats can contribute to variability in assemblages, including species richness and abundance (Figure 5) and influence ecosystem function, forming a mosaic of microhabitats (Levin, 1992; Levin et al., 2016; Portail et al., 2016). The mosaic of habitats at the South Georgia continental shelf may explain the elevated diversity observed in comparison to other infaunal assemblages in the Southern Ocean (Figure 6). An exception to the active methane seep seafloor heterogeneity and microhabitats is the Annenkov Trough - West (AT-W 11) station, where cores cluster together, diverging only between the 0–2 cm and 2–5 cm horizons (Figure 5), suggesting less within-station dissimilarity and a more homogenised seafloor, maybe as a result of the high abundances of Maldanidae polychaetes, in comparison with all other seep stations.

4.2 Species richness and composition at the South Georgia methane seeps

The South Georgia shelf is one of the most biodiverse areas in the Southern Ocean, hosting 40% more species than the neighbouring South Orkney Islands shelf and over three times the density of novel species compared to the Antarctic Peninsula shelf (Hogg et al., 2011). At the South Georgia active methane seep stations, species richness ranged from 19 to 51 species. In contrast, Bell et al. (2016a) reported a narrower range of 34 to 45 species at the Ice Fjord Trough seeps. Other active methane seep environments, such as those in Costa Rica (372–1908 m), exhibited lower species richness, with transitional zones (the area between active and non-active sediments) averaging 18.23 ± 2.26 species and active seep areas at 15.23 ± 3.38 species (Levin et al., 2015). Arctic seeps have shown a range of 9 to 41 species (Åström et al., 2018).

Arthropoda, Annelida and Mollusca were dominant components of the South Georgia methane seeps representing 48% (50 species), 30% (31 species) and 9.7% (10 species, 5 bivalve, 5 gastropod) of total assemblage. In comparison to the seeps, the general South Georgia shelf biodiversity has lower relative richness of Arthropoda (19.6%, 283 species) and Annelida (10%, 147 species) and higher relative richness of Mollusca (11%, 161 species) (Hogg et al., 2011). This suggests an enrichment of arthropods and annelids at the South Georgia methane seeps, and a depauperation of molluscs compared to the broader South Georgia shelf assemblages. Universal taxa from the Southern Ocean comparative sites, found in at least one core per ecosystem, included Amphipoda (ranging from 1.2% at Ice Fjord Trough (IFT) to 4.0% at Hydrothermal Northern Antarctic Peninsula (HT NAP)), Bivalvia (3.6% at HT NAP to 26.6% at the background organic-carbon Northern Antarctic Peninsula (NAP)), Echinodermata (0.1% at IFT to 4.0% at HT NAP), Isopoda (0.1% at IFT to 13% at HT NAP), and Tanaidacea (0.2% at IFT to 9.1% at HT NAP). Notably, the relative abundance patterns of taxa were similar between the active methane seep stations, background Northern Antarctic Peninsula (NAP), and ice-covered Eastern Weddell Sea (EWS). In contrast, the tanaids (5.4%) were prominent at the persistent labile organic matter sediments (FB NAP), while the Hydrothermal Northern Antarctic Peninsula (HT NAP) was characterised by Isopoda (13%) and Tanaidacea (9.1%), suggesting isopods and tanaids thrive in high organic-carbon and hydrothermal environments.

The Annenkov Trough - West (AT-W 11) station had high abundances dominated by annelid species from the families Maldanidae, Ampharetidae, and Lumbrineridae. Maldanidae were absent from four stations, present in low abundances at five stations, and were present in their highest abundances at two stations: they were present in three out of four cores at Royal Trough (RT 14, maximum 382 m^{-2}) and in all cores at the Annenkov Trough - West (AT-W 11, 12,605 m^{-2}). Maldanidae were present at stations with a range of SMT depths, reflecting their known distribution in benthic ecosystems both shallower than and within Oxygen Minimum Zones (OMZs) (Joydas and Damodaran, 2014; Levin et al., 2000). The Annenkov Trough - West, a hydrogen sulfide-influenced station, supports high Maldanidae abundances, consistent with their frequent occurrence in sediments around whale falls (Fujiwara et al., 2007; Smith et al., 2015), cold seeps (Smith et al., 2015), and deep-sea hydrothermal environments, including as a keystone species in Loki's Castle vent field on the Arctic Mid-Ocean Ridge (Kongsrud and Rapp, 2011). Some maldanids at vents and seeps demonstrate a strong reliance on chemosynthetically produced organic matter, and have a high tolerance to sulfides and hypoxia (Jumars et al., 2015). Their abundance was approximately 33 times higher between Royal Trough (RT 14) and Annenkov Trough - West (AT-W 11). This pattern mirrors observations near offshore fish farms, where proximity to organic-rich sediments correlates with higher Maldanidae densities (Riera et al., 2015). This suggests that the Annenkov Trough - West contains higher organically available

carbon than other active methane seep stations, supporting a more abundant Maldanidae assemblage. Ampharetidae were present in only eight of 38 South Georgia cores (five in the 0–2 cm horizon and three in the 2–5 cm horizon), typically appearing in one core per station, except at Royal Trough (RT 14), where they were present in two cores. Their highest abundances were recorded at inner Drygalski Fjord (DF 03) and Annenkov Trough - West (AT-W 11) (354 m^{-2}). As deposit feeders, Ampharetidae are commonly observed at whale falls (Smith et al., 2015) and chemosynthetic environments, including microbial mats, hydrothermal sediments, and background deep-sea sediments (Levin and Dayton, 2009), suggesting a strong sulfide association. Ampharetidae have also been found in sediments at depths above, within, and below OMZs (Joydas and Damodaran, 2014; Levin et al., 2000), suggesting a degree of ecological flexibility that allows them to persist not only in sulfidic and low-oxygen environments but also in adjacent habitats, perhaps explaining their presence across the inner Drygalski Fjord, Royal Trough and Annenkov Trough - West (Jumars et al., 2015). Ampharetidae are an early successional taxa in deep-sea methane seeps, with their tube building actively promoting the growth of bacteria, increasing the flux of methane through the sediment-water interface (Arrázola and Acosta, 2024; Bowden et al., 2013; Cordes et al., 2005, 2006; Sommer et al., 2007; Cordes et al., 2010). Lumbrineridae were only found at two of the 11 stations, at the Royal Trough (RT 14, 127 m^{-2}) and in their highest abundance at the Annenkov Trough - West (AT-W 11, 707 m^{-2}). Lumbrineridae have been recorded in organically enriched but non-sulfidic environments such as inactive hydrothermal sediments (Levin and Dayton, 2009) and sewage outflows, where they exhibit opportunistic behaviour (Vesal et al., 2021). The presence of these three polychaete families at the deeper Annenkov Trough (AT-W 11) aligns with their known associations with high-organic, sulfidic, and microbial mat environments; the station supports a diverse assemblage, likely due to the coexistence of sulfide-associated taxa such as Ampharetidae and more opportunistic taxa like Lumbrineridae.

Five bivalve species were found within the South Georgia methane seeps and included *Propeleda longicaudata* and *Axinulus antarcticus*, a Mysella genus and two Nucula species, five gastropod species were also identified. In the Ice Fjord Trough methane seeps, only four species of Bivalvia: *Propeleda longicaudata, Ennucula* sp., *Mysella antarctica, and Axinulus antarcticus* were found, no gastropods were collected (Bell et al., 2016a). Both this study and the Bell et al. (2016a) documented low bivalve richness at the active methane seep stations with respect to South Georgia's documented bivalve diversity (59 species; Linse, 2014). *Axinulus antarcticus* was present at all stations but three, it was absent from the stations with the deepest SMTs: the inner Drygalski Fjord (DF 03) and both Royal Trough stations (RT 13 and RT 14). *Axinulus antarcticus* is a widely distributed bivalve across the Weddell Gyre region and is a colonising species within the formerly ice-shelf-covered Prince Gustav Channel (Anderson et al., 2021). This suggests that *Axinulus antarcticus* has a broader ecological tolerance and is capable of surviving in recently disturbed environments as a coloniser, as well as in sediments with shallower SMTs. In our study, *Propeleda longicaudata* was found exclusively at the high methane-flux, high surface sediment hydrogen sulfide concentration station of Church Trough (CT 05). Off the coast of Baja California, *Propeleda* sp. were found below an oxygen concentration of 0.2 ml/L, suggesting that this taxon is capable of tolerating hypoxic conditions (Suárez-Mozo et al., 2019). In South Georgia, Nucula species were most abundant at the Royal Trough stations (RT 13 & 14) and were present in high abundance at the Annenkov Trough - West (AT-W 11), this taxa has been recorded in sediments below the extent of the OMZ in the Arabian Sea (Levin et al., 2000) as well as in both active and inactive cold seeps (Levin and Dayton, 2009). Calcifying organisms accounted for 15% of species richness in both this study and Bell et al. (2016a), which is slightly lower than the 20% reported for South Georgia as a whole (Hogg et al., 2011). At the Northern Antarctic Peninsula Hydrothermal Seeps, calcifiers made up an even smaller proportion (13%) of species richness (Bell et al., 2016a),suggesting that seep environments may selectively favour non-calcifying taxa.

The noted absence of vesicomyid clams at all South Georgia methane seep stations was also noted at a whale fall in Monterey Canyon, California (Goffredi et al., 2004). Goffredi et al. (2004) attributed this absence to bathymetric stratification, species depth distributions, and the duration of sulfophilic stage colonisation at the seeps. Vesicomyidae have a depth distribution of 400–7000 m, deeper than all stations in this study (OBIS, 2025). Methane seep assemblages are structured by depth in the Sea of Okhotsk, with chemosynthetic taxa richness decreasing at shallower depths (Sahling et al., 2003); deeper seeps hosted vesicomyid clams, solemyid bivalves, and thyasirids, while shallower stations (~160 m) only contained patchy bacterial mats. Church Trough, which contained the highest hydrogen sulfide concentrations, was the deepest site within the study area but may still be too shallow for those bivalve species to colonise. The Cumberland Bay stations (CB 07, CB 08), the shallowest at 136–142 m, exhibited the lowest abundances and species richness. Seep obligate or symbiont-bearing taxa are often poorly represented or completely absent in shallow-water seeps (Levin, 2005; Sahling et al., 2003). At shallow seeps (<400 m), a greater proportion of photosynthetic production accompanies chemosynthetic production, increasing the potential for more generalist taxa to inhabit these sediments (Åström et al., 2016). The high abundance, high richness station of Annenkov Trough (second deepest station within this study at 358 m), with the coexistence of sulfide-associated taxa, opportunistic and generalist taxa, may be at an optimum depth and suitable hydrogen sulfide concentrations to support taxa with life strategies supported by either or both chemosynthetic and photosynthetic derived organic matter.

4.3 South Georgia methane seep Polychaete families in the context of Southern Ocean soft sediment environments

At the class and family level, the Northern Antarctic Peninsula sediments with persistent labile organic matter (FB NAP) had the highest taxa richness (15–18 taxa). The stations around the

Northern Antarctic Peninsula which we described as having "background" organic-carbon levels (NAP, stations had ice cover ranging from none, irregular, to seasonal (Säring et al., 2022)) had the second highest taxa richness with 9–15 taxa. The South Georgia (SG) methane seep stations had the widest range of taxa richness (5–14 taxa), with the Ice Fjord Trough (IFT) positioned at the median (9 taxa). The lowest taxa richness was observed at the Hydrothermal Northern Antarctic Peninsula (HT NAP) (6–10 taxa) and the ice-covered Eastern Weddell Sea (ice cover described as high and constant (Säring et al., 2022)) (6–8 taxa).

Among polychaete families, Hesionidae was found in every South Georgia core, with the highest abundances at the Annenkov Trough - West (AT-W 11). It was also present in cores in the Ice Fjord Trough (IFT), and in the persistent labile organic sediments (FB NAP) stations and two of the hydrothermal stations (HT NAP). Hesionidae abundance has been shown to increase from background (non-seep) sediments to active seep areas in Costa Rica methane seeps (Ashford et al., 2021a) and is associated with whale falls (Hilario et al., 2015; Silva et al., 2021; Sumida et al., 2016), wood falls (Salazar-Vallejo and Orensanz, 2006; Saeedi et al., 2019), and hydrothermal vents (Kroesche and Rouse, 2025). This indicates that the Family Hesionidae contains a chemosynthetic-associated taxa, commonly found in organic-rich reducing environments and associated with microbial mats (Jumars et al., 2015). Cirratulidae were present at all South Georgia stations, with highest abundances at the outer Drygalski Fjord station (DF 04, 2,457 m-^{2}) and Annenkov Trough - East station (AT-E 12, 4,711 m-^{2}), but lowest abundance at the inner Drygalski Fjord (DF 03, 88 m-^{2}). Higher Cirratulidae abundance has been reported in transitional versus background sediments (transitional sediments are potential ecotone between active methane seeps and non-seep sediments) (Ashford et al., 2021b) which aligns with their presence at the lower methane-flux stations of the outer Drygalski Fjord (DF 04) and Annenkov Trough - East (AT-E 12). In the Ice Fjord Trough three species were identified (Bell et al., 2016a), cirratulids were found at all the persistent labile organic matter sediment stations (FB NAP) and all the Hydrothermal Northern Antarctic Peninsula (HT NAP) stations. They are a taxon known to dominate populations in oxygen minimum zones (Joydas and Damodaran, 2014; Levin et al., 2000) and organic rich sediments at fish farms (Valdemarsen et al., 2015). Cirratulidae are a widespread and opportunistic taxon, exhibiting tolerance to transitional environments, organic-enriched sediments, and low-oxygen conditions. Orbiniidae were present at all South Georgia (SG) stations and three Hydrothermal Northern Antarctic Peninsula (HT NAP) stations but was entirely absent from the Ice Fjord Trough (IFT), persistent labile organic matter sediment stations (FB NAP), and the Costa Rica stations (Ashford et al., 2021b). Orbiniidae are known to dominate microbial mat sediments at cold seeps (Levin and Dayton, 2009) but show increased abundance with distance from organic rich fish farm sediments (Valdemarsen et al., 2015). In a three year whale fall study, it was only present for the first two years (Fujiwara et al., 2007), which indicates that this taxonomic group may be an earlier coloniser of reducing sediments. Terebellids were found across all stations in the Weddell Gyre, Northern Antarctic Peninsula and South Georgia stations, but were notably sparse in the inner Drygalski Fjord station (DF 03). This family has been recorded throughout all three years of whale fall observations (Fujiwara et al., 2007) and occurs both in sediments above (Joydas and Damodaran, 2014) and below oxygen minimum zones (Levin et al., 2000), but not within. Tereblellids have been found to use peloids from bacterial sulfate reduction to construct their tubes (Guido et al., 2017). Terebellids are a cosmopolitan taxon, capable of surviving and feeding in reducing sediments (Jumars et al., 2015). The key polychaete families in South Georgia's methane seeps overlap with those found in sediment-hosted hydrothermal vents, persistent high organic-matter sedimented stations, whale falls, fish farms, oxygen minimum zones, and cold seeps. Their presence and relative abundance suggest distinct ecological preferences, with some taxa favouring more transitional, or early succession sediments while others thrive in high methane- flux or organic-rich conditions.

4.4 The future of Southern Ocean methane seeps

In the future, with warming Antarctic waters (Purkey and Johnson, 2013) melting glaciers and ice sheets, leading to reduced pressure on the continental shelf, the currently stable gas hydrates on the Antarctic shelf will begin to destabilise (Giustiniani et al., 2020). The sub-Antarctic South Georgia, where active methane seeps were detected in the early 2000s, serves as the ideal sentinel for climate change in Antarctica (Graham et al., 2017). Methane is actively degassing on the South Georgia shelf, with an increasing number of detected flare sites (Bohrmann et al., 2017; Workman et al., 2024) and there are signs that geochemical characteristics of the sediment which indicate active methane seeps are having an impact on the macrobenthic assemblages. The assemblage at the South Georgia degassing gas hydrate site showed greater diversity compared to other Southern Ocean sites, potentially reflecting the early stages of seep assemblage development.

Despite these insights, several key uncertainties remain regarding methane seep dynamics in the region. The variability of MUC lengths may influence our understanding of sulfate/methane transition (SMT) depths. SMT depths are typically estimated from sulfate depletion profiles, and shorter MUC cores may not have fully captured the extent of sulfate depletion, potentially overestimating the depth at which methane oxidation occurs. Additionally, the role of macrofauna in modifying SMT depths is known to occur at other seeps, including the impact of larger vesicomyid clams, for example, which can extend the SMT deeper into the sediment through their biological activity, subsequently isolating smaller, less mobile organisms from the sulfide source (Fischer et al., 2012). The observed differences in assemblage composition between the Annenkov Trough - West (AT-W 11) and Church Trough (CT 05) suggest that Annenkov Trough may represent a more advanced stage of seep succession, with higher richness, abundance and key chemosynthetic taxa, including the presence of known methane seep polychaete taxa. Investigating how

seep-associated fauna shape SMT depth and methane flux over time will be critical to refining our understanding of methane seep succession in Southern Ocean environments. To date, the stability (e.g., methane fluxes) and life expectancy of these seeps remain unknown, as do their temporal dynamics on daily, seasonal, and interannual scales, and their impact on benthic metazoan, functional traits, and trophodynamics. Studying these questions at South Georgia methane seeps will address key knowledge gaps in seep succession within Southern Ocean waters. Understanding these processes will not only provide insights into the impacts of active methane seeps on benthic ecosystems but also serve as a proxy for predicting changes in Antarctic continental shelf sediments due to gas hydrate destabilisation and the broader consequences for Antarctic benthic biodiversity.

Data availability statement

The datasets presented in this study can be found in online repositories. The names of the repository/repositories and accession number(s) can be found in the article/Supplementary Material.

Author contributions

MA: Conceptualization, Data curation, Formal Analysis, Investigation, Methodology, Project administration, Software, Validation, Writing – original draft, Writing – review & editing. WR: Funding acquisition, Project administration, Supervision, Visualization, Writing – original draft, Writing – review & editing. GB: Funding acquisition, Project administration, Resources, Writing – review & editing. ID: Investigation, Methodology, Writing – review & editing. PH: Supervision, Writing – review & editing. SK: Conceptualization, Data curation, Investigation, Methodology, Writing – review & editing. TP: Conceptualization, Data curation, Investigation, Writing – review & editing. MR: Conceptualization, Data curation, Investigation, Writing – review & editing. JN: Supervision, Writing – review & editing. BW: Supervision, Writing – review & editing. KL: Conceptualization, Data curation, Funding acquisition, Investigation, Project administration, Resources, Supervision, Validation, Writing – review & editing.

Funding

The author(s) declare financial support was received for the research and/or publication of this article. The fieldwork for this study, including participation of GB, TP and MR, was supported by the Deutsche Forschungsgemeinschaft (DFG) in the framework of the priority program 'Antarctic Research with comparative investigations in Arctic ice areas' by project-id 40464014, and within the DFG-Research Center/Cluster of Excellence EXC 309 "The Ocean in the Earth System" through project-id 49926684. The expedition under the title "Emissions of free gas around South Georgia: distribution, quantification, and sources for methane ebullition sites in sub-Antarctic waters" was carried out with the support of MARUM -Center for Marine Environmental Sciences, Research Faculty University of Bremen and the University of Bremen. We also acknowledge support from the Helmholtz Association (Alfred Wegener Institute Helmholtz Centre for Polar and Marine Research, Bremerhaven). The cruise was sponsored by the German Research Foundation (DFG) and by the Federal Ministry of Education and Research (BMBF). Katrin Linse is part of the British Antarctic Survey Polar Science for Planet Earth Programme (NC Science), funded by The Natural Environment Research Council (NERC). Studies around South Georgia were undertaken under permit RAP 129/2016 (M134) issued by the Foreign & Commonwealth Office, UK. Macrobenthic faunal sorting to morphotaxon level was supported by the Natural Environment Research Council via a DEI Internship for Madeline PBC Anderson (via the NERC Diversity, Equity and Inclusion (DEI) engagement funding). This work was supported by the Natural Environment Research Council via an IAPETUS2 PhD studentship held by Madeline PBC Anderson (grant reference NE/S007431/1).

Acknowledgments

We are grateful for the support by the master and crews of RV METEOR expedition M134. We thank Klaus Dehning and Daniel Hütting (both MARUM, University of Bremen) for their technical support to the MUC system, Susan Mau (Faculty of Geoscience, University of Bremen) and Torben Gentz (Alfred Wegener Institute Helmholtz Centre for Polar and Marine Research, Bremerhaven) for carrying out the CTD measurements, and Oliver Hogg for sample slicing and sieving support. We acknowledge the team of the ROV MARUM-SQUID for providing *in-situ* imagery from methane seepage sites. Anne Helene Tandberg, Magdalena Blażewic, Saskia Brix and Regan Drennan are thanked for their help with peracarid and annelid identifications. Janice Malnati (Faculty of Geoscience, University of Bremen) is thanked for assistance with sediment sampling and methane concentration analysis.

Conflict of interest

The authors declare that the research was conducted in the absence of any commercial or financial relationships that could be construed as a potential conflict of interest.

Generative AI statement

The author(s) declare that no Generative AI was used in the creation of this manuscript.

Any alternative text (alt text) provided alongside figures in this article has been generated by Frontiers with the support of artificial intelligence and reasonable efforts have been made to ensure

accuracy, including review by the authors wherever possible. If you identify any issues, please contact us.

Publisher's note

All claims expressed in this article are solely those of the authors and do not necessarily represent those of their affiliated organizations, or those of the publisher, the editors and the reviewers. Any product that may be evaluated in this article, or claim that may be made by its manufacturer, is not guaranteed or endorsed by the publisher.

Supplementary material

The Supplementary Material for this article can be found online at: https://www.frontiersin.org/articles/10.3389/fmars.2025.1589660/full#supplementary-material

References

Anderson, M. (2025). M134-SG-assemblage-manuscript-scripts: release: V1.0.Zenodo. doi: 10.5281/zenodo.14983251

Anderson, M. P. B. C., Fenberg, P. B., Griffiths, H. J., and Linse, K. (2021). *Macrobenthic Mollusca of the Prince Gustav Channel* Vol. 8 (Eastern Antarctic Peninsula: An Area Undergoing Colonisation.Frontiers in Marine Science).

Anderson, M., Pape, T., and Linse, K. (2025). *Macrobenthic assemblages from the methane seeps in six South Georgia troughs collected in 2017 (Version 1.0) [Data set}* (Madingley Road, Cambridge: NERC EDS UK Polar Data Centre). doi: 10.5285/d34fc0d7-3ef5-49df-b626-908d76e28f75

Arntz, W. E., and Rauschert, M. (2015). Antarctic macrobenthos: a field guide of the invertebrates living at the Antarctic seafloor. doi: 10.1007/s00300-016-1905-2

Arrázola, J., and Acosta, A. (2024). Conceptual representation of the life cycle of methane seep ecosystems. *Mar. Biol. Res.* 20 (9-10), 380–400. doi: 10.1080/17451000.2024.2392740

Ashford, O. S., Guan, S., Capone, D., Rigney, K., Rowley, K., Cordes, E. E., et al. (2021a). Relationships between biodiversity and ecosystem functioning proxies strengthen when approaching chemosynthetic deep-sea methane seeps. *Proc. R. Soc. B: Biol. Sci.* 288, 20210950. doi: 10.1098/rspb.2021.0950

Ashford, O. S., Guan, S., Capone, D., Rigney, K., Rowley, K., Orphan, V., et al. (2021b). A chemosynthetic ecotone—"chemotone"—in the sediments surrounding deep-sea methane seeps. *Limnol Oceanog* 66, 1687–1702. doi: 10.1002/lno.11713

Åström, E. K. L., Carroll, M. L., Ambrose, W. G., and Carroll, J. (2016). Arctic cold seeps in marine methane hydrate environments: impacts on shelf macrobenthic community structure offshore Svalbard. *Mar. Ecol. Prog. Ser.* 552, 1–18. doi: 10.3354/meps11773

Åström, E. K. L., Carroll, M. L., Ambrose, W. G., Sen, A., Silyakova, A., and Carroll, J. (2018). Methane cold seeps as biological oases in the high-Arctic deep sea: Cold seeps in the high-Arctic deep sea. *Limnol Oceanog* 63, S209–S231. doi: 10.1002/lno.10732

Åström, E. K. L., Carroll, M. L., Sen, A., Niemann, H. C., Ambrose, W. G., Lehmann, M. F., et al. (2019). Chemosynthesis influences food web and community structure in high-Arctic benthos. *Mar. Ecol. Prog. Ser.* 629, 19–42. doi: 10.3354/meps13101

Åström, E. K. L., Sen, A., Carroll, M. L., and Carroll, J. (2020). Cold seeps in a warming arctic: insights for benthic ecology. *Front. Mar. Sci.* 7, 244. doi: 10.3389/fmars.2020.00244

Barry, J. P., Gary Greene, H., Orange, D. L., Baxter, C. H., Robison, B. H., Kochevar, R. E., et al. (1996). Biologic and geologic characteristics of cold seeps in Monterey Bay, California. *Deep Sea Res. Part I: Oceanog Res. Papers* 43, 1739–1762. doi: 10.1016/s0967-0637(96)00075-1

Belchier, M. (2004). "FPRV dorada cruise DOSG04: south Georgia groundfish survey, 6th january - 10th february 2004," in *A report to the Government of the South Georgia and the South Sandwich Islands*.

Bell, J. B., Aquilina, A., Woulds, C., Glover, A. G., Little, C. T. S., Reid, W. D. K., et al. (2016a). Geochemistry, faunal composition and trophic structure in reducing sediments on the southwest South Georgia margin. *R. Soc. Open Sci.* 3, 160284. doi: 10.1098/rsos.160284

Bell, J. B., Brown, L. E., Sweeting, C. J., Reid, W. D. K., Little, C. T. S., Glover, A. G., et al. (2016b). Macrofaunal ecology of sedimented hydrothermal vents in the bransfield strait, Antarctica. *Front. Mar. Sci.* 3. doi: 10.3389/fmars.2016.00032

Bernardino, A. F., Levin, L. A., Thurber, A. R., and Smith, C. R. (2012). Comparative composition, diversity and trophic ecology of sediment macrofauna at vents, seeps and organic falls. *PLoS One* 733515. doi: 10.1371/journal.pone.0033515

Boetius, A., Ravenschlag, K., Schubert, C. J., Rickert, D., Widdel, F., Gieseke, A., et al. (2000). A marine microbial consortium apparently mediating anaerobic oxidation of methane. *Nature* 407, 623–626. doi: 10.1038/35036572

Bohrmann, G. (2013). The expedition of the research vessel 'Polarstern' to the antarctic in 2013 (ANT-XXIX/4). doi: 10.2312/BzPM_0668_2013

Bohrmann, G., Aromokeye, A. D., Bihler, V., Dehning, K., Dohrmann, I., Gentz, T., et al. (2017). R/V METEOR cruise report M134, emissions of free gas from cross-shelf troughs of south Georgia: distribution, quantification, and sources for methane ebullition sites in sub-antarctic waters, port stanley (Falkland islands) - punta arenas (Chile), 16 january - 18 february 2017. doi: urn:nbn:de:gbv:46-00106081-12

Bohrmann, G., Heeschen, K., Jung, C., Weinrebe, W., Baranov, B., Cailleau, B., et al. (2002a). Widespread fluid expulsion along the seafloor of the Costa Rica convergent margin. *Terra Nova* 14, 69–79. doi: 10.1046/j.1365-3121.2002.00400.x

Bohrmann, G., Suess, E., Greinert, J., Teichert, B., and Naehr, T. (2002b). Gas Hydrate Carbonates from Hydrate Ridge, Cascadia Convergent Margin: Indicators of near-seafloor clathrate deposits. doi: 10.1029/GM124p0099

Bowden, D. A., Rowden, A. A., Thurber, A. R., Baco, A. R., Levin, L. A., and Smith, C. R. (2013). Cold seep epifaunal communities on the hikurangi margin, New Zealand: composition, succession, and vulnerability to human activities. *PloS One* 8, e76869. doi: 10.1371/journal.pone.0076869

Bray, J. R., and Curtis, J. T. (1957). An ordination of the upland forest communities of southern wisconsin. *Ecol. Monogr.* 27, 326–349. doi: 10.2307/1942268

Cline, J. D. (1969). Spectrophotometric determination of hydrogen sulfide in natural waters 1. *Limnology and Oceanography*, 14 (3), 454–458.

Cordes, E. E., Arthur, M. A., Shea, K., Arvidson, R. S., and Fisher, C. R. (2005). Modeling the mutualistic interactions between tubeworms and microbial consortia. *PloS Biol.* 3, e77. doi: 10.1371/journal.pbio.0030077

Cordes, E. E., Bergquist, D. C., Predmore, B. L., Jones, C., Deines, P., Telesnicki, G., et al. (2006). Alternate unstable states: Convergent paths of succession in hydrocarbon-seep tubeworm-associated communities. *J. Exp. Mar. Biol. Ecol.* 339, 159–176. doi: 10.1016/j.jembe.2006.07.017

Cordes, E. E., Carney, S. L., Hourdez, S., Carney, R. S., Brooks, J. M., and Fisher, C. R. (2007). Cold seeps of the deep Gulf of Mexico: Community structure and biogeographic comparisons to Atlantic equatorial belt seep communities. *Deep Sea Res. Part I: Oceanog Res. Papers* 54, 637–653. doi: 10.1016/j.dsr.2007.01.001

Cordes, E. E., Cunha, M. R., Galéron, J., Mora, C., Olu-Le Roy, K., Sibuet, M., et al. (2010). The influence of geological, geochemical, and biogenic habitat heterogeneity on seep biodiversity. *Mar. Ecol.* 31 (1), 51–65. doi: 10.1111/j.1439-0485.2009.00334.x

De Beer, D., Sauter, E., Niemann, H., Kaul, N., Foucher, J.-P., Witte, U., et al. (2006). *In situ* fluxes and zonation of microbial activity in surface sediments of the Håkon Mosby Mud Volcano. *Limnol Oceanog* 51, 1315–1331. doi: 10.4319/lo.2006.51.3.1315

del Valle, R. A., Yermolin, E., Chiarandini, J., Sanchez Granel, A., and Lusky, J. C. (2017). Methane at the NW of weddell sea, Antarctica. *J. Geol Res.* 2017, 5952916. doi: 10.1155/2017/5952916

Dorschel, B., Hehemann, L., Viquerat, S., Warnke, F., Dreutter, S., Schulze Tenberge, Y., et al. (2022). The international bathymetric chart of the southern ocean version 2 (IBCSO v2). *Scientific Data*. 9, 275. doi: 10.1038/s41597-022-01366-7

Ferré, B., Mienert, J., and Feseker, T. (2012). Ocean temperature variability for the past 60 years on the Norwegian-Svalbard margin influences gas hydrate stability on human time scales. *J. Geophys Res: Oceans* 117 (C10). doi: 10.1029/2012JC008300

Fischer, D., Mogollón, J. M., Strasser, M., Pape, T., Bohrmann, G., Fekete, N., et al. (2013). Subduction zone earthquake as potential trigger of submarine hydrocarbon seepage. *Nat. Geosci.* 6, 647–651. doi: 10.1038/ngeo1886

Fischer, D., Sahling, H., Nöthen, K., Bohrmann, G., Zabel, M., and Kasten, S. (2012). Interaction between hydrocarbon seepage, chemosynthetic communities, and bottom water redox at cold seeps of the Makran accretionary prism: insights from habitat-specific pore water sampling and modeling. *Biogeosciences* 9, 2013–2031. doi: 10.5194/bg-9-2013-2012

Fujiwara, Y., Kawato, M., Yamamoto, T., Yamanaka, T., Sato-Okoshi, W., Noda, C., et al. (2007). Three-year investigations into sperm whale-fall ecosystems in Japan. *Mar. Ecol.* 28, 219–232. doi: 10.1111/j.1439-0485.2007.00150.x

Geprägs, P., Torres, M. E., Mau, S., Kasten, S., Römer, M., and Bohrmann, G. (2016). Carbon cycling fed by methane seepage at the shallow Cumberland Bay, South Georgia, sub-Antarctic: METHANE SEEPAGE IN CUMBERLAND BAY. *Geochem Geophys Geosyst* 17, 1401–1418. doi: 10.1002/2016GC006276

Giustiniani, M., Tinivella, U., Giustiniani, M., and Tinivella, U. (2020). "Gas hydrates in Antarctica," in *Glaciers and the Polar Environment* (London, United Kingdom: IntechOpen).

Glover, A. G., Smith, C. R., Mincks, S. L., Sumida, P. Y. G., and Thurber, A. R. (2008). Macrofaunal abundance and composition on the West Antarctic Peninsula continental shelf: Evidence for a sediment "food bank" and similarities to deep-sea habitats. *Deep Sea Res. Part II: Topical Stud. Oceanog* 55, 2491–2501. doi: 10.1016/j.dsr2.2008.06.008

Goffredi, S. K., Paull, C. K., Fulton-Bennett, K., Hurtado, L. A., and Vrijenhoek, R. C. (2004). Unusual benthic fauna associated with a whale fall in Monterey Canyon, California. *Deep Sea Res. Part I: Oceanog Res. Papers* 51, 1295–1306. doi: 10.1016/j.dsr.2004.05.009

Graham, A. G. C., Kuhn, G., Meisel, O., Hillenbrand, C.-D., Hodgson, D. A., Ehrmann, W., et al. (2017). Major advance of South Georgia glaciers during the Antarctic Cold Reversal following extensive sub-Antarctic glaciation. *Nat. Commun.* 8, 14798. doi: 10.1038/ncomms14798

Guido, A., Rosso, A., Sanfilippo, R., Russo, F., and Mastandrea, A. (2017). Microbial biomineralization in biotic crusts from a pleistocene marine cave (NW Sicily, Italy). *Geomicrobiol J.* 34, 864–872. doi: 10.1080/01490451.2017.1284283

Hall, P. O. J., and Aller, R. C. (1992) Rapid, small-volume, flow injection analysis for ΣCO2 and NH4+ in marine and freshwaters. *Limnology and Oceanograpy*, 37, 1113–1119.

Henning, C. (2024). fpc: flexible procedures for clustering. doi: 10.32614/CRAN.package.fpc

Hilario, A., Cunha, M. R., Génio, L., Marçal, A. R., Ravara, A., Rodrigues, C. F., et al. (2015). First clues on the ecology of whale falls in the deep Atlantic Ocean: results from an experiment using cow carcasses. *Mar. Ecol.* 36, 82–90. doi: 10.1111/maec.12246

Hinrichs, K.-U., Hayes, J. M., Sylva, S. P., Brewer, P. G., and DeLong, E. F. (1999). Methane-consuming archaebacteria in marine sediments. *Nature* 398, 802–805. doi: 10.1038/19751

Hodgson, D. A., Graham, A. G. C., Griffiths, H. J., Roberts, S. J., Cofaigh, C.Ó., Bentley, M. J., et al. (2014). Glacial history of sub-Antarctic South Georgia based on the submarine geomorphology of its fjords. *Quater Sci. Rev.* 89, 129–147. doi: 10.1016/j.quascirev.2013.12.005

Hoehler, T. M., Alperin, M. J., Albert, D. B., and Martens, C. S. (1994). Field and laboratory studies of methane oxidation in an anoxic marine sediment: Evidence for a methanogen-sulfate reducer consortium. *Global Biogeochem Cycles* 8, 451–463. doi: 10.1029/94GB01800

Hogg, O. T., Barnes, D. K. A., and Griffiths, H. J. (2011). Highly diverse, poorly studied and uniquely threatened by climate change: an assessment of marine biodiversity on south Georgia's continental shelf' Simon thrush (ed.). *PloS One* 6, e19795. doi: 10.1371/journal.pone.0019795

Hogg, O., Huevenne, V., Griffiths, H., Dorschel, B., and Linse, K. (2015). A bathymetric compilation of south Georgia 1985-2015. doi: 10.5285/ce8bf6be-4b5f-454c-9165-73ab4c3baf23

Iversen, N., and Jorgensen, B. B. (1985). Anaerobic methane oxidation rates at the sulfate-methane transition in marine sediments from Kattegat and Skagerrak (Denmark). *Limnol Oceanog* 30, 944–955. doi: 10.4319/lo.1985.30.5.0944

Joydas, T. V., and Damodaran, R. (2014). Infaunal macrobenthos of the oxygen minimum zone on the Indian western continental shelf. *Mar. Ecol.* 35, 22–35. doi: 10.1111/maec.12052

Joye, S. B. (2020). The geology and biogeochemistry of hydrocarbon seeps. *Annu. Rev. Earth Planet Sci.* 48, 205–231. doi: 10.1146/annurev-earth-063016-020052

Judd, A. G. (2003). *The global importance and context of methane escape from the seabed* (23(3: Geo-Marine Letters), 147–154.

Jumars, P. A., Dorgan, K. M., and Lindsay, S. M. (2015). Diet of worms emended: an update of polychaete feeding guilds. *Annu. Rev. Mar. Sci.* 7, 497–520. doi: 10.1146/annurev-marine-010814-020007

Kongsrud, J. A., and Rapp, H. T. (2011). Nicomache (Loxochona) lokii sp. nov. (Annelida: Polychaeta: Maldanidae) from the Loki's Castle vent field: an important structure builder in an Arctic vent system. *Polar Biol.* 35, 161–170. doi: 10.1007/s00300-011-1048-4

Kroesche, R., and Rouse, G. W. (2025). Four new species of hesionidae (Annelida, polychaeta, phyllodocida) from eastern pacific chemosynthetic habitats and reinstatement of vrijenhoekia. *Diversity* 17, 121. doi: 10.3390/d17020121

Kvenvolden, K. A. (1986). Methane hydrates and global climate. *Science*, 234 (4777), 689–691. doi: 10.1029/GB002i003p00221

Legendre, P., and Gallagher, E. D. (2001). Ecologically meaningful transformations for ordination of species data. *Oecologia* 129, 271–280. doi: 10.1007/s004420100716

Lešić, N.-M., Streuff, K. T., Bohrmann, G., Kasten, S., and Kuhn, G. (2024). Spatial and temporal variability in Holocene trough-fill sediments, King Haakon Trough System, sub-Antarctic South Georgia. *Quater Sci. Adv.* 13, 100156. doi: 10.1016/j.qsa.2023.100156

Lešić, N.-M., Streuff, K. T., Bohrmann, G., and Kuhn, G. (2022). Glacimarine sediments from outer Drygalski Trough, sub-Antarctic South Georgia – evidence for extensive glaciation during the Last Glacial Maximum. *Quater Sci. Rev.* 292, 107657. doi: 10.1016/j.quascirev.2022.107657

Levin, S. A. (1992). The problem of pattern and scale in ecology: the robert H. MacArthur Award Lecture. *Ecology* 73, 1943–1967. doi: 10.2307/1941447

Levin, L. A. (2005). "Ecology of cold seep sediments: interactions of fauna with flow, chemistry and microbes," in *Oceanography and Marine Biology* (Francis Group in Boca Raton, Florida, USA: CRC Press).

Levin, L. A., Baco, A. R., Bowden, D. A., Colaco, A., Cordes, E. E., Cunha, M. R., et al. (2016). Hydrothermal vents and methane seeps: rethinking the sphere of influence. *Front. Mar. Sci.* 3. doi: 10.3389/fmars.2016.00072

Levin, L. A., and Dayton, P. K. (2009). Ecological theory and continental margins: where shallow meets deep. *Trends Ecol. Evol.* 24, 606–617. doi: 10.1016/j.tree.2009.04.012

Levin, L. A., Gage, J. D., Martin, C., and Lamont, P. A. (2000). Macrobenthic community structure within and beneath the oxygen minimum zone, NW Arabian Sea. *Deep Sea Res. Part II: Topical Stud. Oceanog* 47, 189–226. doi: 10.1016/S0967-0645(99)00103-4

Levin, L. A., Mendoza, G. F., Gonzalez, J. P., Thurber, A. R., and Cordes, E. E. (2010). Diversity of bathyal macrofauna on the northeastern Pacific margin: the influence of methane seeps and oxygen minimum zones. *Mar. Ecol.* 31, 94–110. doi: 10.1111/j.1439-0485.2009.00335.x

Levin, L. A., Mendoza, G. F., Grupe, B. M., Gonzalez, J. P., Jellison, B., Rouse, G., et al. (2015). Biodiversity on the rocks: macrofauna inhabiting authigenic carbonate at Costa Rica methane seeps. *PloS One* 10, e0131080. doi: 10.1371/journal.pone.0131080

Levin, L. A., Ziebis, W., Mendoza, G. F., Growney, V. A., Tryon, M. D., Brown, K. M., et al. (2003). Spatial heterogeneity of macrofauna at northern California methane seeps: influence of sulfide concentration and fluid flow. *Mar. Ecol. Prog. Ser.* 265, 123–139. doi: 10.3354/meps265123

Lichtschlag, A., Felden, J., Brüchert, V., Boetius, A., and de Beer, D. (2010). Geochemical processes and chemosynthetic primary production in different thiotrophic mats of the Håkon Mosby Mud Volcano (Barents Sea). *Limnol Oceanog* 55, 931–949. doi: 10.4319/lo.2010.55.2.0931

Linse, K. (2014). "Chapter 5.11. Bivalvia," in *Biogeographic Atlas of the Southern Ocean* (Scientific Committee on Antarctic Research, Cambridge), 126–128.

Linse, K., Sigwart, J. D., Chen, C., and Krylova, E. M. (2020). Ecophysiology and ecological limits of symbiotrophic vesicomyid bivalves (Pliocardiinae) in the Southern Ocean. *Polar Biol.* 43, 1423–1437. doi: 10.1007/s00300-020-02717-z

Magurran, A. E. (2003). "Google-books-ID: cxRSEAAAQBAJ," in *Measuring Biological Diversity* (Chichester, West Sussex, England: John Wiley & Sons).

Mazzini, A., Ivanov, M. K., Nermoen, A., Bahr, A., Bohrmann, G., Svensen, H., et al. (2008). Complex plumbing systems in the near subsurface: Geometries of authigenic carbonates from Dolgovskoy Mound (Black Sea) constrained by analogue experiments. *Mar. Petroleum Geol* 25, 457–472. doi: 10.1016/j.marpetgeo.2007.10.002

Montagna, P. A., Baguley, J. G., Hsiang, C.-Y., and Reuscher, M. G. (2017). Comparison of sampling methods for deep-sea infauna: Sampling methods for deep-sea infauna. *Limnol Oceanog: Methods* 15, 166–183. doi: 10.1002/lom3.10150

Myhre, C. L., Ferré, B., Platt, S. M., Silyakova, A., Hermansen, O., Allen, G., et al. (2016). Extensive release of methane from Arctic seabed west of Svalbard during summer 2014 does not influence the atmosphere. *Geophys Res. Lett.* 43, 4624–4631. doi: 10.1002/2016GL068999

Nakayama, C. R., Kuhn, E., Araújo, A. C. V., Alvalá, P. C., Ferreira, W. J., Vazoller, R. F., et al. (2011). Revealing archaeal diversity patterns and methane fluxes in Admiralty Bay, King George Island, and their association to Brazilian Antarctic Station activities. *Deep Sea Res. Part II: Topical Stud. Oceanog* 58, 128–138. doi: 10.1016/j.dsr2.2010.10.013

Niemann, H., Fischer, D., Graffe, D., Knittel, K., Montiel, A., Heilmayer, O., et al. (2009). Biogeochemistry of a low-activity cold seep in the Larsen B area, western Weddell Sea, Antarctica. *Biogeosciences* 6, 2383–2395. doi: 10.5194/bg-6-2383-2009

Niewöhner, C., Hensen, C., Kasten, S., Zabel, M., and Schulz, H. D. (1998). Deep sulfate reduction completely mediated by anaerobic methane oxidation in sediments of the upwelling area off Namibia. *Geochim Cosmochim Acta* 62 (3), 455–464. doi: 10.1016/S0016-7037(98)00055-6

Nöthen, K., and Kasten, S. (2011). Reconstructing changes in seep activity by means of pore water and solid phase Sr/Ca and Mg/Ca ratios in pockmark sediments of the Northern Congo Fan. *Mar. Geol* 287, 1–13. doi: 10.1016/j.margeo.2011.06.008

OBIS (2025). *Vesicomyidae dall & C. T. Simpson 1901 - ocean biodiversity information system*. Available online at: https://obis.org/taxon/as23140 (Accessed February 21, 2025).

Oksanen, J., Simpson, G. L., Blanchet, F. G., Kindt, R., Legendre, P., Minchin, P. R., et al. (2024). vegan: community ecology package. doi: 10.32614/CRAN.package.vegan

Olu, K., Decker, C., Pastor, L., Caprais, J.-C., Khripounoff, A., Morineaux, M., et al. (2017). Cold-seep-like macrofaunal communities in organic- and sulfide-rich sediments of the Congo deep-sea fan. *Deep Sea Res. Part II: Topical Stud. Oceanog* 142, 180–196. doi: 10.1016/j.dsr2.2017.05.005

Pape, T., Geprägs, P., Hammerschmidt, S., Wintersteller, P., Wei, J., Fleischmann, T., et al. (2014). Hydrocarbon seepage and its sources at mud volcanoes of the Kumano forearc basin, Nankai Trough subduction zone. Geochemistry, Geophysics, *Geosystems*, 15 (6), 2180–2194. doi: 10.1002/2013GC005057

Pielou, E. C. (1966). The measurement of diversity in different types of biological collections. *J. Theor. Biol.* 13, 131–144. doi: 10.1016/0022-5193(66)90013-0

Portail, M., Olu, K., Dubois, S. F., Escobar-Briones, E., Gelinas, Y., Menot, L., et al. (2016). Food-web complexity in guaymas basin hydrothermal vents and cold seeps. *PloS One* 11, e0162263. doi: 10.1371/journal.pone.0162263

Portail, M., Olu, K., Escobar-Briones, E., Caprais, J. C., Menot, L., Waeles, M., et al. (2015). Comparative study of vent and seep macrofaunal communities in the Guaymas Basin. *Biogeosciences* 12, 5455–5479. doi: 10.5194/bg-12-5455-2015

Portnov, A., Vadakkepuliyambatta, S., Mienert, J., and Hubbard, A. (2016). Ice-sheet-driven methane storage and release in the Arctic. *Nat. Commun.* 7, 10314. doi: 10.1038/ncomms10314

Purkey, S. G., and Johnson, G. C. (2013). Antarctic bottom water warming and freshening: contributions to sea level rise, ocean freshwater budgets, and global heat gain. *J. Climate* 26, 6105–6122. doi: 10.1175/JCLI-D-12-00834.1

R Core Team (2024). *R: A Language and Environment for Statistical Computing*. Vienna, Austria.

Riera, R., Tuya, F., Pérez, Ó., Ramos, E., Rodríguez, M., and Monterroso, Ó. (2015). Effects of proximity to offshore fish farms over soft-bottom macrofauna. *J. Mar. Biol. Assoc. U Kingdom* 95, 255–263. doi: 10.1017/S0025315414001386

Römer, M., Sahling, H., Pape, T., Bahr, A., Feseker, T., Wintersteller, P., et al. (2012). Geological control and magnitude of methane ebullition from a high-flux seep area in the Black Sea—the Kerch seep area. *Mar. Geol* 319–322, 57–74. doi: 10.1016/j.margeo.2012.07.005

Römer, M., Sahling, H., Pape, T., dos Santos Ferreira, C., Wenzhöfer, F., Boetius, A., et al. (2014a). Methane fluxes and carbonate deposits at a cold seep area of the Central Nile Deep Sea Fan, Eastern Mediterranean Sea. *Mar. Geol* 347, 27–42. doi: 10.1016/j.margeo.2013.10.011

Römer, M., Torres, M., Kasten, S., Kuhn, G., Graham, A. G. C., Mau, S., et al. (2014b). First evidence of widespread active methane seepage in the Southern Ocean, off the sub-Antarctic island of South Georgia. *Earth Planet Sci. Lett.* 403, 166–177. doi: 10.1016/j.epsl.2014.06.036

Saeedi, H., Bernardino, A. F., Shimabukuro, M., Falchetto, G., and Sumida, P. Y. G. (2019). Macrofaunal community structure and biodiversity patterns based on a wood-fall experiment in the deep South-west Atlantic. *Deep Sea Res. Part I: Oceanog Res. Papers* 145, 73–82. doi: 10.1016/j.dsr.2019.01.008

Sahling, H., Galkin, S. V., Salyuk, A., Greinert, J., Foerstel, H., Piepenburg, D., et al. (2003). Depth-related structure and ecological significance of cold-seep communities—a case study from the Sea of Okhotsk. *Deep Sea Res. Part I: Oceanog Res. Papers* 50, 1391–1409. doi: 10.1016/j.dsr.2003.08.004

Sahling, H., Rickert, D., Lee, R. W., Linke, P., and Suess, E. (2002). Macrofaunal community structure and sulfide flux at gas hydrate deposits from the Cascadia convergent margin, NE Pacific. *Mar. Ecol. Prog. Ser.* 231, 121–138. doi: 10.3354/meps231121

Salazar-Vallejo, S. I., and Orensanz, J. M. (2006). Pleijelius longae n. gen., n. sp., a remarkable deep water polychaete from the Northwestern Atlantic (Polychaeta: Hesionidae). *Scie Marina* 70, 157–165. doi: 10.3989/scimar.2006.70s3157

Säring, F., Seifert, D., Baumann, M., and Link, H. (2021a). Macrofauna abundance from multicorer and box corer samples for ten stations around the Antarctic Peninsula (POLARSTERN cruise PS 81, ANT-XXIX/3, January–March 2013). doi: 10.1594/PANGAEA.932693

Säring, F., Seifert, D., and Link, H. (2021b). Macrofauna abundance from multicorer and box corer samples for seven stations from the Weddell Sea (POLARSTERN cruise PS 96, ANT-XXXI/2, December 2015–February 2016). doi: 10.1594/PANGAEA.932658

Säring, F., Veit-Köhler, G., Seifert, D., Liskow, I., and Link, H. (2022). Sea-ice-related environmental drivers affect meiofauna and macrofauna communities differently at large scales (Southern Ocean, Antarctic). *Mar. Ecol. Prog. Ser.* 700, 13–37. doi: 10.3354/meps14188

Schnakenberg, A., Aromokeye, D. A., Kulkarni, A., Maier, L., Wunder, L. C., Richter-Heitmann, T., et al. (2021). Electron acceptor availability shapes anaerobically methane oxidizing archaea (ANME) communities in south Georgia sediments. *Front. Microbiol.* 12, 617280. doi: 10.3389/fmicb.2021.617280

Seeberg-Elverfeldt, J., Schlüter, M., Feseker, T., and Kölling, M. (2005). Rhizon sampling of porewaters near the sediment-water interface of aquatic systems. *Limnol. Oceanogr. Methods* 3, 361–371. doi: 10.4319/lom.2005.3.361

Shannon, C. E. (1948). A mathematical theory of communication. *Bell Syst. Tech. J.* 27, 379–423 & 623–656. doi: 10.1002/j.1538-7305.1948.tb00917.x

Silva, A. P., Colaço, A., Ravara, A., Jakobsen, J., Jakobsen, K., and Cuvelier, D. (2021). The first whale fall on the Mid-Atlantic Ridge: Monitoring a year of succession. *Deep Sea Res. Part I: Oceanog Res. Papers* 178, 103662. doi: 10.1016/j.dsr.2021.103662

Simpson, E. H. (1949). Measurement of diversity. *Nature* 163, 688–688. doi: 10.1038/163688a0

Smith, C. R., Glover, A. G., Treude, T., Higgs, N. D., and Amon, D. J. (2015). Whale-fall ecosystems: recent insights into ecology, paleoecology, and evolution. *Annu. Rev. Mar. Sci.* 7, 571–596. doi: 10.1146/annurev-marine-010213-135144

Sommer, S., Gutzmann, E., and Pfannkuche, O. (2007). Sediments hosting gas hydrate: oases for metazoan meiofauna. *Mar. Ecol. Prog. Ser.* 337, 27–37. doi: 10.3354/meps337027

Sommer, S., Linke, P., Pfannkuche, O., Niemann, H., and Treude, T. (2010). Benthic respiration in a seep habitat dominated by dense beds of ampharetid polychaetes at the Hikurangi Margin (New Zealand). *Mar. Geol* 272, 223–232. doi: 10.1016/j.margeo.2009.06.003

Stocker, T. F., Qin, D., Plattner, G.-K., Tignor, M. M. B., Allen, S. K., Boschung, J., et al. (2014). "Climate change 2013: the physical science basis," in *Contribution of Working Group I to the Fifth Assessment Report of IPCC the Intergovernmental Panel on Climate Change*. Eds. T. Stocker, D. Qin, G.-K. Plattner, M. Tignor, S. Allen, J. Boschung, A. Nauels, Yu Xia, V. Bex and P. Midgley (Cambridge University Press, Cambridge).

Stolper, D. A., Lawson, M., Davis, C. L., Ferreira, A. A., Neto, E. V. S., Ellis, G. S., et al. (2014). Formation temperatures of thermogenic and biogenic methane. *Science* 344, 1500–1503. doi: 10.1126/science.1254509

Streuff, K. T., Lešić, N.-M., Kuhn, G., Römer, M., Kasten, S., and Bohrmann, G. (2024). Glacial history of the King Haakon trough system, sub-Antarctic South Georgia. *Quater Sci. Rev.* 338, 108749. doi: 10.1016/j.quascirev.2024.108749

Suárez-Mozo, N. Y., Valentich-Scott, P., and Hendrickx, M. E. (2019). Deep-water bivalves from the oxygen minimum zone area off the western Peninsula of Baja California, Mexico. *Molluscan Res.* 39, 99–109. doi: 10.1080/13235818.2018.1508550

Sumida, P. Y. G., Alfaro-Lucas, J. M., Shimabukuro, M., Kitazato, H., Perez, J. A. A., Soares-Gomes, A., et al. (2016). Deep-sea whale fall fauna from the Atlantic resembles that of the Pacific Ocean. *Sci. Rep.* 6, 22139. doi: 10.1038/srep22139

Taillefert, M., Beckler, J. S., Cathalot, C., Michalopoulos, P., Corvaisier, R., Kiriazis, N., et al. (2017). Early diagenesis in the sediments of the Congo deep-sea fan dominated by massive terrigenous deposits: Part II – Iron–sulfur coupling. *Deep Sea Res. Part II: Topical Stud. Oceanog* 142, 151–166. doi: 10.1016/j.dsr2.2017.06.009

Thurber, A. R., Levin, L. A., Rowden, A. A., Sommer, S., Linke, P., and Kröger, K. (2013). Microbes, macrofauna, and methane: A novel seep community fueled by aerobic methanotrophy. *Limnol Oceanog* 58, 1640–1656. doi: 10.4319/lo.2013.58.5.1640

Thurber, A. R., Seabrook, S., and Welsh, R. M. (2020). Riddles in the cold: Antarctic endemism and microbial succession impact methane cycling in the Southern Ocean. *Proc. R. Soc. B: Biol. Sci.* 287, 20201134. doi: 10.1098/rspb.2020.1134

Torres, M. E., McManus, J., Hammond, D. E., de Angelis, M. A., Heeschen, K. U., Colbert, S. L., et al. (2002). Fluid and chemical fluxes in and out of sediments hosting methane hydrate deposits on Hydrate Ridge, OR, I: Hydrological provinces. *Earth Planet Sci. Lett.* 201, 525–540. doi: 10.1016/S0012-821X(02)00733-1

Treude, T., Niggemann, J., Kallmeyer, J., Wintersteller, P., Schubert, C. J., Boetius, A., et al. (2005). Anaerobic oxidation of methane and sulfate reduction along the Chilean continental margin. *Geochim Cosmochim Acta* 69, 2767–2779. doi: 10.1016/j.gca.2005.01.002

Valdemarsen, T., Hansen, P. K., Ervik, A., and Bannister, R. J. (2015). Impact of deep-water fish farms on benthic macrofauna communities under different hydrodynamic conditions. *Mar. pollut. Bull.* 101, 776–783. doi: 10.1016/j.marpolbul.2015.09.036

Vesal, S. E., Nasi, F., Pazzaglia, J., Ferrante, L., Auriemma, R., Relitti, F., et al. (2021). Assessing the sewage discharge effects on soft-bottom macrofauna through traits-based approach. *Mar. pollut. Bull.* 173, 113003. doi: 10.1016/j.marpolbul.2021.113003

Vetter, E. W., and Dayton, P. K. (1998). Macrofaunal communities within and adjacent to a detritus-rich submarine canyon system. *Deep Sea Res. Part II: Topical Stud. Oceanog* 45, 25–54. doi: 10.1016/S0967-0645(97)00048-9

Wallmann, K., Linke, P., Suess, E., Bohrmann, G., Sahling, H., Schlüter, M., et al. (1997). Quantifying fluid flow, solute mixing, and biogeochemical turnover at cold vents of the eastern Aleutian subduction zone. *Geochim Cosmochim Acta* 61, 5209–5219. doi: 10.1016/S0016-7037(97)00306-2

Washburn, T. W., Demopoulos, A. W. J., and Montagna, P. A. (2018). Macrobenthic infaunal communities associated with deep-sea hydrocarbon seeps in the northern Gulf of Mexico. *Mar. Ecol.* 39, 12508. doi: 10.1111/maec.12508

Whiticar, M. J. (1999). Carbon and hydrogen isotope systematics of bacterial formation and oxidation of methane. *Chem. Geol* 161, 291–314. doi: 10.1016/S0009-2541(99)00092-3

Whiticar, M. J., and Suess, E. (1990). Hydrothermal hydrocarbon gases in the sediments of the King George Basin, Bransfield Strait, Antarctica. *Appl. Geochem* 5, 135–147. doi: 10.1016/0883-2927(90)90044-6

Wickham, H., Averick, M., Bryan, J., Chang, W., McGowan, L. D., François, R., et al. (2019). Welcome to the {tidyverse}. *J. Open Source Software* 4, 1686. doi: 10.21105/joss.01686

Workman, E., Fisher, R. E., France, J. L., Linse, K., Yang, M., Bell, T., et al. (2024). Methane emissions from seabed to atmosphere in polar oceans revealed by direct methane flux measurements. *J. Geophys Res: Atmospheres* 129, e2023JD040632. doi: 10.1029/2023JD040632

Wunder, L. C., Aromokeye, D. A., Yin, X., Richter-Heitmann, T., Willis-Poratti, G., Schnakenberg, A., et al. (2021). Iron and sulfate reduction structure microbial communities in (sub-)Antarctic sediments. *ISME J.* 15, 3587–3604. doi: 10.1038/s41396-021-01014-9

Young, E. F., Meredith, M. P., Murphy, E. J., and Carvalho, G. R. (2011). High-resolution modelling of the shelf and open ocean adjacent to South Georgia, Southern Ocean. *Deep Sea Res. Part II: Topical Stud. Oceanog* 58, 1540–1552. doi: 10.1016/j.dsr2.2009.11.003

Zanker, J. C., Young, E., Holland, P. R., Haigh, I. D., and Brickle, P. (2024). Oceanographic variability in cumberland bay, south Georgia, and its implications for glacier retreat. *J. Geophys Res: Oceans* 129, e2023JC020507. doi: 10.1029/2023JC020507